High-statistics study of the reactions $\pi^- p \to K^- K^+ n$ and $\pi^+ n \to K^- K^+ p$ at 6 GeV/c*

A. J. Pawlicki, D. S. Ayres, D. Cohen, R. Diebold, S. L. Kramer, and A. B. Wicklund
Argonne National Laboratory, Argonne, Illinois 60439
(Received 23 December 1976; revised manuscript received 15 March 1977)

The Argonne Effective Mass Spectrometer has been used for a high-precision study of the reactions $\pi^- p \to K^- K^+ n$ (110 000 events) and $\pi^+ n \to K^- K^+ p$ (50 000 events) at 6 GeV/c for $K^- K^+$ masses below 1750 MeV and momentum transfers $-t < 0.40$ GeV^2. Comparison of the two reactions isolates interferences between isospin-0 and isospin-1 $K^- K^+$ states. We observe f-A_2^0, f'-A_2^0, and f-f' interferences in the Y_4^0 moment and find f' production to have a substantial contribution from some mechanism other than pion exchange. We present values for the f' mass (1506 ± 5 MeV), width (66 ± 10 MeV), and branching ratio $[(f' \to \pi\pi / f' \to \text{all}) = (1.2 \pm 0.4)\%]$. The relative f-f' production phase is found to be 170 ± 10°; the 2^{++} nonet mixing angle is determined to be 32.5 ± 0.5°, which is less than the ideal value. The measured relative f-A_2^0 production phase of $(63^{+11}_{-15})°$ confirms a prediction of Irving and Michael based on duality and vector-meson production studies. The $\bar{K}K$ branching ratio of the f meson is measured to be $(f \to \bar{K}K / f \to \text{all}) = (3.8 \pm 0.4)\%$. An SU(3) prediction for the ratio of the ρKK to the $\rho\pi\pi$ coupling is found to agree with the data. In addition to the isospin-0 S*, substantial isospin-1 S-wave production is observed near the $K^- K^+$ threshold and the effects of the recently reported S-wave enhancement of mass ~1300 MeV are observed. Our results show that the enhancement has isospin 0, with a slow variation of phase.

I. INTRODUCTION

We report high-statistics measurements of the mass and momentum-transfer dependence of the $K^- K^+$ decay angular distribution moments in the reactions

$$\pi^- p \to K^- K^+ n \quad (110\,000 \text{ events}), \tag{1}$$

$$\pi^+ n \to K^- K^+ p \quad (50\,000 \text{ events}). \tag{2}$$

The $K^- K^+$ mass range from threshold to 1750 MeV is covered, for the four-momentum transfer range $-t < 0.40$ GeV^2. Heretofore, no systematic comparison of reactions (1) and (2) has been made. The largest statistical samples previously available for reaction (1) have 16 000 events[1] and 27 000 events.[2] For the related reaction,

$$\pi^- p \to K_S^0 K_S^0 n\,, \tag{3}$$

the largest existing samples for which moments have been measured have about 6000 events[3-5] each.

Lipkin[6] has pointed out that if A_0 and A_1 are the amplitudes for production of $I = 0$ and $I = 1$ $K^- K^+$ systems in reaction (1), then the amplitude for reaction (1) is $A_0 + A_1$, while for the reaction $\pi^- p \to \bar{K}^0 K^0 n$ the amplitude is $A_0 - A_1$. By charge independence this amplitude is the same as that for reaction (2), and apart from a factor $1/\sqrt{2}$ the even partial-wave amplitudes are the same for reaction (3), which has no odd partial waves. Symbolically we can write the cross sections for reactions (1) and (2) as

$$\sigma^{\mp} = |A_0 \pm A_1|^2 = |A_0|^2 + |A_1|^2 \pm 2\,\mathrm{Re}(A_0 A_1^*)\,,$$

where we have defined $d^2\sigma/dt\,dM \equiv \sigma\langle Y_0^0\rangle = \sigma/(4\pi)^{1/2}$, M is the $K^- K^+$ effective mass, t is the four-momentum transfer to the recoil nucleon, and the superscripts − and + refer to reactions (1) and (2), respectively. Using the standard symbols for meson states to represent the various amplitudes, we can write

$$\sigma^{\mp} = |S^* \pm \delta^0|^2 + |\phi \pm \rho^0|^2 + |f + f' \pm A_2^0|^2 + \cdots\,.$$

Summing the two cross sections eliminates the $A_0 A_1^*$ interference terms; taking the difference isolates those terms. Similar relations hold for the various $K^- K^+$ decay moments; for example, the contributions of the three tensor mesons to the Y_4^0 moment are, symbolically,

$$\sigma_{\mathrm{sum}}\langle Y_4^0\rangle \propto |f|^2 + |f'|^2 + |A_2^0|^2 + 2\,\mathrm{Re}(f f'^*)\,,$$

$$\sigma_{\mathrm{dif}}\langle Y_4^0\rangle \propto \mathrm{Re}(f A_2^{0*}) + \mathrm{Re}(f' A_2^{0*})\,.$$

Here

$$\sigma_{\mathrm{sum}}\langle Y_l^m\rangle \equiv \sigma^-\langle Y_l^m\rangle + \sigma^+\langle Y_l^m\rangle$$

and

$$\sigma_{\mathrm{dif}}\langle Y_l^m\rangle \equiv \sigma^-\langle Y_l^m\rangle - \sigma^+\langle Y_l^m\rangle$$

(the $\langle Y_l^m\rangle$ are defined in Sec. II).

The quantum numbers of $\bar{K}K$ systems are greatly restricted. Two pseudoscalar mesons can only form natural-parity systems, i.e., with parity and spin related by $P = (-1)^J$. The statistics of a boson-antiboson pair further require $C = P$, and this leads to $G = C(-1)^I = (-1)^{I+J}$ (Ref. 7). In general, we expect the cross section at small t to be dominated by one-pion exchange (OPE), which can only produce $\bar{K}K$ systems with even-G parity, such as S*(993), ρ(770), f(1270), g(1680), etc. Since these

states have $I+J=$ even, $\sigma_{\text{sum}} \langle Y^m_{\text{odd}} \rangle$ and $\sigma_{\text{dif}} \langle Y^m_{\text{even}} \rangle$ would be zero if OPE were the only production mechanism. While these moments are indeed small relative to the cross section at low t, many of them are nonzero and are a measure of the interference of odd-G-parity amplitudes with the dominant OPE amplitudes. To the extent that OPE is well understood,[8,9] we can use it as a probe to study the odd-G-parity amplitudes.

In a previous experiment[1] we found an excess of events in the 1400- to 1500-MeV region for reaction (1). Although we explained most of this excess in terms of large constructive f-A_2^0 interference, this explanation predicted a depletion of events for reaction (3) in the same mass range. This was at variance with a previous experiment[3] which also observed an excess of $K_S^0 K_S^0$ events in this region. With high statistics for both reactions (1) and (2), the present experiment showed that this effect is in fact due to f-f' interference.[10] This was the first observation of the f' in pion-induced reactions. The f' production is strongly suppressed in these reactions, as expected from the Iizuka-Okubo-Zweig rule[11]; the severity of the suppression is about the same as that of $\phi \to \rho\pi$.[12] The f' width of 66 ± 10 MeV measured in this experiment is larger than the world average[13] of 40 ± 10 MeV, but is in good agreement with recent measurements[14,15] of 61 ± 8 MeV and 62^{+19}_{-14} MeV.

In addition to sorting out the f, f', and A_2^0 D-wave contributions, the comparison of reactions (1) and (2) revealed the presence of a significant $I=1$ (and hence non-OPE) S wave near K^-K^+ threshold, along with the large $I=0$ S^* effect. This is of interest for coupled-channel analysis of $\pi\pi \to \pi\pi$ and $\pi\pi \to \bar{K}K$; previous work[16] treated the low-mass K^-K^+ S wave as purely $I=0$. At higher masses, the effects of a recently discovered S-wave enhancement[5] with mass ~1300 MeV and width ~150 MeV were observed, and the isospin assignment of the enhancement was shown to be $I=0$. In the P waves, the ϕ meson was observed while the $I=1$ P wave was found to be consistent with the tail of the ρ^0 meson for $M < 1400$ MeV.

The experimental method is outlined in Sec. II. The data are presented in Sec. III and their gross features are briefly discussed. Section IV contains detailed analyses of various features of the data, while Sec. V summarizes the results of the experiment.

II. EXPERIMENTAL METHOD

A. Description of the apparatus and trigger requirements

Data were taken at 6-GeV/c incident beam momentum using the Argonne Effective Mass Spectrometer. The spectrometer configuration and trigger logic requirements were similar to those of an earlier experiment[1,12,17] which studied reaction (1). Additional information about the spectrometer is given in Ref. 18. The apparatus is shown in Fig. 1. Pions in the unseparated beam were identified by threshold Čerenkov counters; a scintillation-counter hodoscope measured the beam momentum to $\pm 0.27\%$ and the incident beam direction at the target was measured to ± 1 mrad by the $K0$ chambers. The HOLE and dE/dx coun-

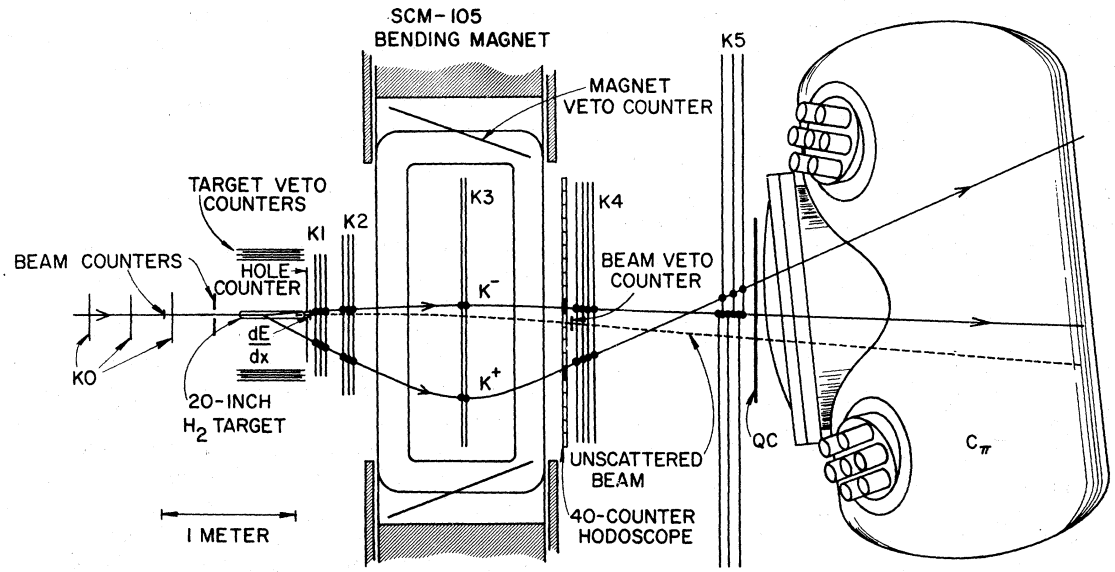

FIG. 1. Plan view of the Argonne Effective Mass Spectrometer. $K0$ through $K5$ are sets of magnetostrictive-readout wire-spark chambers. C_π is a Freon-filled threshold Čerenkov counter.

ters were used in the trigger to detect interactions of interest in the 50-cm liquid hydrogen or deuterium target; one or more large-angle particles striking the HOLE counter or at least two particles through the dE/dx counter were required. Noninteracting beam triggers were further suppressed by the beam veto counter. The trigger also required two and only two counts in the 40-counter hodoscope at the magnet exit. Events with fast charged pions ($p_\pi \gtrsim 1.5$ GeV/c) were suppressed by the large Čerenkov counter, C_π[19]; the counter QC ensured that at least one charged particle entered C_π. The spectrometer magnet had a gap of 66 cm, a width of 2 m, an effective length of 1 m, and $\int Bdl = 11.4$ kG m. The sets of magnetostrictive wire spark chambers, $K1$ through $K5$, measured the trajectories of outgoing particles. Data were recorded on magnetic tape by an EMR 6050 computer, which also analyzed a sample of the data on-line.

For reaction (1), unwanted final states such as $K^-K^+\Delta^0$ were suppressed in the trigger logic by rejecting events accompanied by a count in any one of the target veto counters (which surrounded the target on four sides and included both charged-particle and γ-ray counters) or in any of the magnet veto counters (charged-particle counters which lined the upstream half of the magnet aperture). For reaction (2), the presence of a recoil proton required a somewhat looser trigger: the γ-ray veto counters were not used and an event was vetoed only if either (a) two or more of the charged-particle veto counters counted, or (b) either of the magnet veto counters immediately above or below the beam region counted. The status of all the veto counters was recorded for each triggering event for use during data analysis.

B. Trigger losses

A $\pi N \to K^-K^+N$ event in which both kaons traversed the spectrometer and at least one kaon struck the QC counter could still fail to trigger the apparatus. There were a number of loss mechanisms for which we corrected our data.

1. The requirement of two and only two counts in the 40-counter hodoscope at the magnet exit caused a $(4.4 \pm 0.5)\%$ loss of good events that gave three or more counts; this was measured by special data runs with the trigger modified to require at least three hodoscope counts. There was also a loss of $(1.6 \pm 0.8)\%$ of good events with fewer than two hodoscope counts, due to small gaps between adjacent hodoscope elements. Another mechanism for having only one hodoscope count was for both kaons to strike the same hodoscope element; this effect was included in the apparatus acceptance calculation.

2. The recoil neutrons from reaction (1) had a probability $\lesssim 10\%$ of converting in the target veto counters; this effect had a smooth dependence on M and t and was included in the apparatus acceptance calculation.

3. No correction was made for vetoing of events by the spectator proton in $\pi^+d \to K^-K^+pp_s$ because it was determined in a previous experiment[20] that the spectator proton in $\pi^+d \to \pi^-\pi^+pp_s$ was detected by the veto counter array for less than 1% of the events.

4. A good event was lost if one beam particle passed through the beam veto counter in coincidence with a good event initiated by another beam particle. This effect was continuously measured by recording coincidences of beam signals delayed 70 ns (one accelerator rf period) with in-time beam signals. An average correction of $\sim 2\%$ was made.

5. δ rays from the passage of the incident pion and outgoing kaons through liquid hydrogen veto $\sim 6\%$ of good events. This effect was included in the apparatus acceptance calculation.

6. The large threshold Čerenkov counter C_π, which suppressed final states such as $\pi^-\pi^+n$ in the trigger, also had a small efficiency (typically 5 to 10%) for vetoing high-momentum kaons from very asymmetric decays of high-mass ($M > 1475$ MeV) K^-K^+ systems. This effect, as well as the effects of kaon interactions and $K \to \mu\nu$ decays inside the large C_π volume, was included in the apparatus acceptance calculation.

7. An event was lost if the K^- or K^+ struck the beam veto counter; this effect was included in the apparatus acceptance calculation.

8. Loss of events due to absorption of outgoing kaons in spectrometer material or liquid hydrogen or deuterium was included in the apparatus acceptance calculation.

C. Event selection criteria

In the analysis of those events recorded by the apparatus, a number of selection criteria were imposed.

1. Two and only two tracks through the spectrometer magnet were required, resulting in a loss of $(6 \pm 4)\%$ of good events due to spark-chamber and reconstruction program inefficiencies. There was no apparent K^-K^+N signal in the event sample with three tracks through the spectrometer.

2. For reaction (1), an event was rejected if an extra track upstream of the magnet was detected in the $K1$ and $K2$ chambers; for reaction (2), such tracks were acceptable only if they were consistent with the expected recoil proton direction. This cut

caused a loss of $(0.50 \pm 0.25)\%$ of good events, while reducing the background from high-multiplicity final states. The loss was determined from the K^-K^+N signal in the sample of rejected events.

3. For reaction (2), any veto counter recorded as counting must have been consistent with the expected recoil proton direction; otherwise the event was rejected. This requirement caused a loss of $(2.0 \pm 1.5)\%$ of good events.

4. Only one beam track was permitted in the $K0$ chambers. Typically 2% of good events were lost due to this requirment. The effect depended on beam intensity and was measured as the probability of having two reconstructed beam tracks for "beam trigger" events. These were events, recorded continuously throughout the data-taking, for which the event trigger was simply the beam signature part of the full trigger logic.

5. At least one track of momentum ≥ 1.6 GeV/c was required to enter the C_π fiducial volume, to guarantee efficient vetoing of pions. This requirement was also used in defining the apparatus acceptance.

6. Both tracks through the spectrometer magnet had to be inside the magnet's fiducial aperture and had to miss the beam veto counter's fiducial aperture. These aperture cuts were included in the definition of the acceptance.

7. If the two tracks through the spectrometer yielded an apparent $K^+\pi^-$ effective mass of 840 to 960 MeV, the event was rejected so that $K^{*0}Y^0$ final states were excluded. (This was done only for events with apparent K^-K^+ effective mass $M > 1240$ MeV; below 1240 MeV, kinematic resolution was sufficient to exclude $K^{*0}Y^0$ events.) Similarly, an apparent $p\pi^-$ mass within 6 MeV of the Λ mass caused rejection of the event, independent of K^-K^+ mass. Corrections for these cuts were included in the acceptance calculation.

The overall normalization uncertainty, due to uncertainties in spectrometer and reconstruction program efficiencies and absolute pion beam flux, is estimated to be $\pm 10\%$.

D. Kinematic cuts and background corrections

Each event passing the above selection criteria was analyzed assuming that a particle-anti particle pair was produced with a recoil nucleon, i.e., that the reaction was of the type $\pi^- p \to A^- A^+ n$ [$\pi^+ n \to A^- A^+ p$ for reaction (2)]. The mass squared of A, M_A^2, was then calculated; some of the resulting distributions are shown in Fig. 2. Large K^-K^+N signals are evident. Figure 3 shows raw effective mass spectra for reactions (1) and (2) for a cut on the K^-K^+N peak of $|M_A^2 - M_K^2| < 0.15$ GeV^2. In these plots, total backgrounds are ~20%, but are mass dependent.

The M_A^2 distributions have been fitted as the sum of three contributions: a K^-K^+N Gaussian signal, a $\pi^-\pi^+X$ contribution from the small fraction of such events not vetoed by the C_π counter, and a second-order polynomial which parameterized all other background effects, including, for example, the resolution-smeared tails of the $K^-K^+N^*$ and $K^-K^+\Delta$ contributions at large M_A^2.

The background due to $\pi^-\pi^+X$ events for which C_π failed to count is well understood because data were also recorded using a trigger without the C_π veto requirement (C_π-OUT data). After being subjected to the same event selection as the K^-K^+N data (C_π-IN data), the C_π-OUT events were divided into three categories, depending on the probability that C_π would have failed to veto the events. In category (a), both tracks passed the C_π momentum and fiducial volume cuts; since C_π had an inefficiency of only 1.8% per pion track, a negligible number of $\pi^-\pi^+X$ events of this type occurred in the C_π-IN data. In category (b), one track passed the C_π cuts while the second failed, but still could count in C_π with reduced efficiency (if it were a pion). In category (c), one track passed the C_π cuts while the other (if a pion) had negligible efficiency for counting in C_π. Only categories (b) and (c) events were significant contaminants in the C_π-IN data. For C_π-OUT events in each category [(b) or (c)] separately, the M_A^2 distribution was fitted to the sum of a $\pi^-\pi^+N$ Gaussian and second-order polynomial. The M_A^2 distribution for C_π-IN events in the corresponding category was then fitted to the sum of a K^-K^+N Gaussian, a multiple of the C_π-OUT spectrum shape, and a polynomial. The parameter multiplying the C_π-OUT spectrum gave the C_π inefficiency for $\pi^-\pi^+X$ events in the category; for category (b) it was $(1.3 \pm 0.2)\%$, while for (c) it was $(1.8 \pm 0.2)\%$ (essentially the inefficiency for single pions).

To perform the background subtraction, we (i) defined two regions of M_A^2, the "peak" region ($|M_A^2 - M_K^2| < 0.14$ GeV^2) and the "control" region ($0.20 < M_A^2 - M_K^2 < 0.30$ GeV^2); (ii) assumed that each of the three contributions to the C_π-IN data had the same K^-K^+ decay angular distribution in the peak as in the control region; (iii) assumed that the $\pi^-\pi^+$ X contribution in each category [(b) or (c)] separately in the C_π-IN data had the same $\pi^-\pi^+$ decay angular distributions as did the corresponding C_π-OUT data. The decay moments were then calculated for four data samples: (1) C_π-IN events passing the peak cut; (2) C_π-IN events in the control region; (3) C_π-OUT category (b) events passing the peak cut; (4) C_π-OUT category (c) events passing the peak cut. We ob-

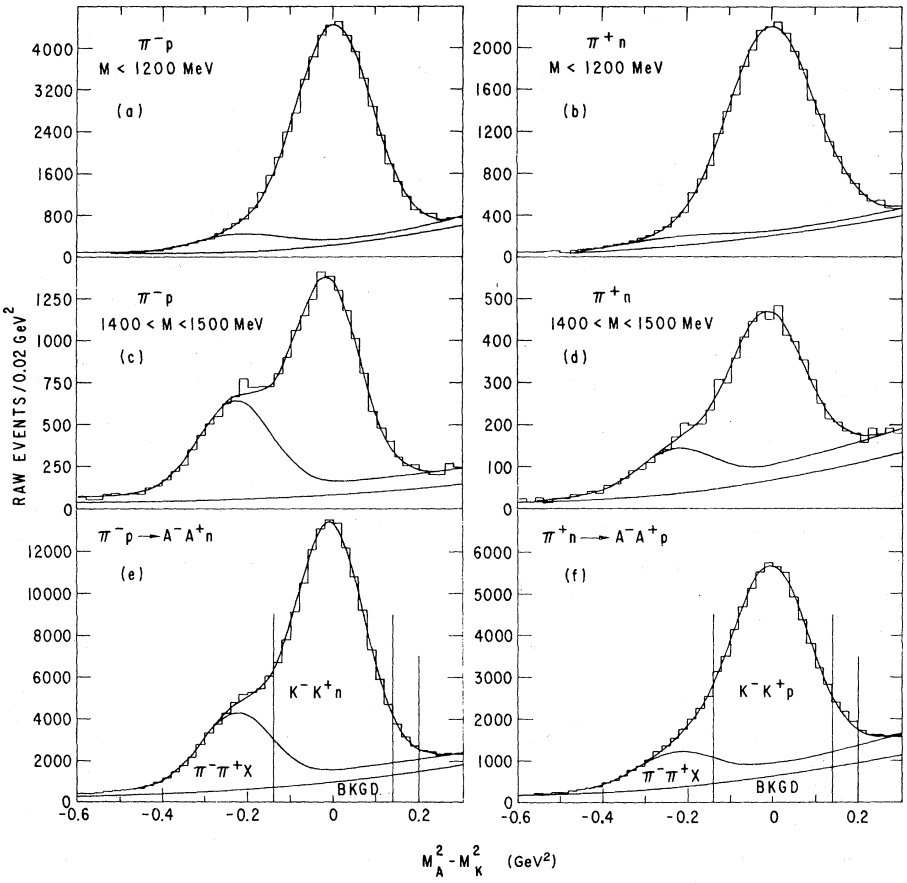

FIG. 2. $M_A{}^2 - M_K{}^2$ distributions for reactions (1) and (2) in several K^-K^+ mass ranges [(a)–(d)] and for the total data samples [(e), (f)]. The vertical lines in (e) and (f) show the K^-K^+ peak cut and the control region cut of 0.2 to 0.3 GeV^2. No t cut has been applied.

tained the background-corrected K^-K^+N moments after subtracting the background moments and correcting for the loss (< 15%) of K^-K^+N events falling outside the peak-region cut. The uncertainty in the $\pi^-\pi^+X$ correction was much smaller than the K^-K^+N statistical uncertainty. The fitted polynomial background inside the K^-K^+N peak cut was typically 15 to 20% in $\sigma\langle Y_0^0\rangle$ and < 10% of $\sigma\langle Y_4^0\rangle$. The parameterization used may overestimate the non-$\pi^-\pi^+X$ background, leading to a systematic uncertainty of ~10% of $\sigma\langle Y_0^0\rangle$ and $\lesssim 5\%$ of $\sigma\langle Y_4^0\rangle$. No corrections have been made for radiative effects (estimated in Ref. 4 to be a loss of ~6%) due to photon emission giving a sufficient energy loss to place events outside the $M_A{}^2$ cuts. Such systematic effects will to first order be common to reactions (1) and (2).

The above procedure was followed in each of several broad M bands to allow for slight variation of $M_A{}^2$ resolution and variation of the character of the backgrounds with K^-K^+ mass. Figure 2 shows $M_A{}^2$ spectra for two M regions, as well as for the total data samples for reactions (1) and (2). The π^+n spectra have somewhat poorer $M_A{}^2$ resolution due to Fermi motion in deuterium.

For each event, the K^-K^+ effective mass M and four-momentum transfer t to the recoil nucleon were determined in a one-constraint fit to the hypothesis of reaction (1) or (2). For each bin in M and t, the moments of the K^-K^+ decay angular distribution were calculated in the t-channel (Jackson) frame. The moments were calculated using the maximum likelihood method described in Ref. 1, which included the effects of spectrometer acceptance. The normalized spherical harmonic moments $\langle Y_l^m\rangle$ are defined by the relation

$$\frac{d^4\sigma}{dt\,dM\,d\Omega} = \sum_{l=0}^{l_{\max}} \sum_{m=-l}^{l} \langle Y_l^m\rangle \,\mathrm{Re}\, Y_l^m(\Omega) \frac{d^2\sigma}{dt\,dM}, \quad (4)$$

where $\Omega = (\cos\theta, \varphi)$ and θ, φ are the angles defining the K^- direction in the t-channel frame.

E. Corrections for deuterium effects

Several effects due to the use of a deuteron target had to be taken into account to obtain data on reaction (2) from measurements of $\pi^+ d \to K^- K^+ p p_s$.

As mentioned in Sec. II B, vetoing by the spectator proton was at the $\lesssim 1\%$ level and no correction was made for this effect.

The effects of liquid-deuterium density (0.1642 g/cm^3) [vs liquid hydrogen (0.0708g/cm^3)] on interaction rate and on absorption of outgoing particles were taken into account appropriately.

Pauli-exclusion-principle effects arise at small t due to the presence of two protons in the final state. A correction factor $[1 - S(\Delta)/3]^{-1}$ has been applied[20-24] to all the moments, where $S(\Delta)$ is the deuteron form factor ($\Delta^2 = -t$). This correction is appropriate for all but the nucleon-helicity-nonflip cross sections for natural-parity exchange, which should vanish as $t \to t_{\min}$ by angular momentum conservation[20] and thus contribute little in the t range where $S(\Delta)$ is large.

An earlier experiment[20] with the same apparatus measured $\pi^- p \to \pi^- \pi^+ n$ and $\pi^+ n \to \pi^- \pi^+ p$ in the ρ^0 region in order to study ρ-ω interference in the $\pi^- \pi^+$ mass spectra. By charge symmetry, these two reactions should have identical cross sections for $\pi^- \pi^+$ masses away from the ω mass, allowing a check on the analysis method for deuterium target data. After the above Pauli-exclusion-principle correction was applied, the cross sections agreed to better than 5%. Empirically, it was found that a Glauber screening correction was not needed, although a 3% Glauber correction also gave acceptable agreement. From Ref. 24, one might expect an effect of $\lesssim 5\%$; we have applied no screening correction to reaction (2) and estimate the possible normalization error due to neglect of spectator-proton vetoing and Glauber screening is less than 5%.

III. RESULTS

The final moments for reactions (1) and (2), corrected for backgrounds, are shown in Figs. 4 to 21 as functions of M and t in the t-channel frame.[25] The sums and differences of the moments for reactions (1) and (2) are also shown. The results for reaction (1) are in agreement with our earlier, lower-statistics study.[1] The cross sections for reactions (1) and (2) for mass <1600 MeV and $-t < 0.4$ GeV^2 are 21.5 μb and 28.2 μb, respectively, with common systematic normalization uncertainty of $\pm 10\%$ and relative uncertainty $\pm 5\%$.

As mentioned in Sec. I, in the limit that the only $K^- K^+$ states are those produced by one-pion exchange (OPE), $\sigma_{\text{sum}} \langle Y^m_{\text{odd}} \rangle = 0$ and $\sigma_{\text{dif}} \langle Y^m_{\text{even}} \rangle = 0$; Figs. 4 to 21 show this behavior as an approximate general trend, but significant deviations abound, indicating some production of odd-G-parity $K^- K^+$ states, especially away from $t = 0$. For example, the cross section for reaction (2), $\sigma^+ \langle Y^0_0 \rangle$, is larger than that for reaction (1), $\sigma^- \langle Y^0_0 \rangle$, for all $M < 1350$ MeV, $-t < 0.4$ GeV^2, as shown in Fig. 4.

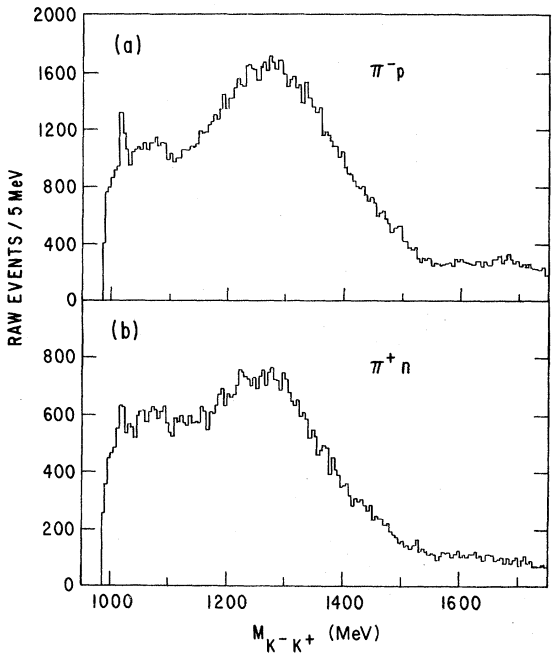

FIG. 3. Raw $K^- K^+$ effective mass distributions for reactions (1) and (2) for $|M_A^2 - M_K^2| < 0.15$ GeV^2 (a slightly tighter cut, 0.14 GeV^2, was used for final event selection). No t cut has been applied.

We also note that the $m = 0$ moments dominate over those with $m = 1$, while the $m = 2$ moments are generally smaller still. These general features have been observed[8] in studies of $\pi^- \pi^+$ systems produced by OPE in $\pi^- p \to \pi^- \pi^+ n$, for $-t < 0.15$ GeV^2.

The moments calculated and shown in Figs. 4 to 21 are those which previous experience[1-5, 8] with $\pi^- \pi^+$ and $K^- K^+$ systems has shown to be different from zero, namely, $m \leq 2$ up to $l = 4$ and $m \leq 1$ for $l = 5$ to 7. The $m = 2$ moments $\langle Y^2_l \rangle$ are omitted for $l \geq 5$ since the spin ≥ 3 amplitudes responsible for these moments are only significant at high M, where limited statistics preclude observing such small effects as $m = 2$ moments.

The slopes B of $\sigma \langle Y^0_0 \rangle$ and $\sigma \langle Y^0_4 \rangle$ resulting from Ae^{Bt} fits to these moments for various mass ranges and $-t \leq 0.2$ GeV^2 are shown in Table I and Fig. 22. As was found in Ref. 1, the slope B_0^- of $\sigma^- \langle Y^0_0 \rangle$ decreases from 16 GeV^{-2} near threshold to 9 GeV^{-2} at 1500 MeV.

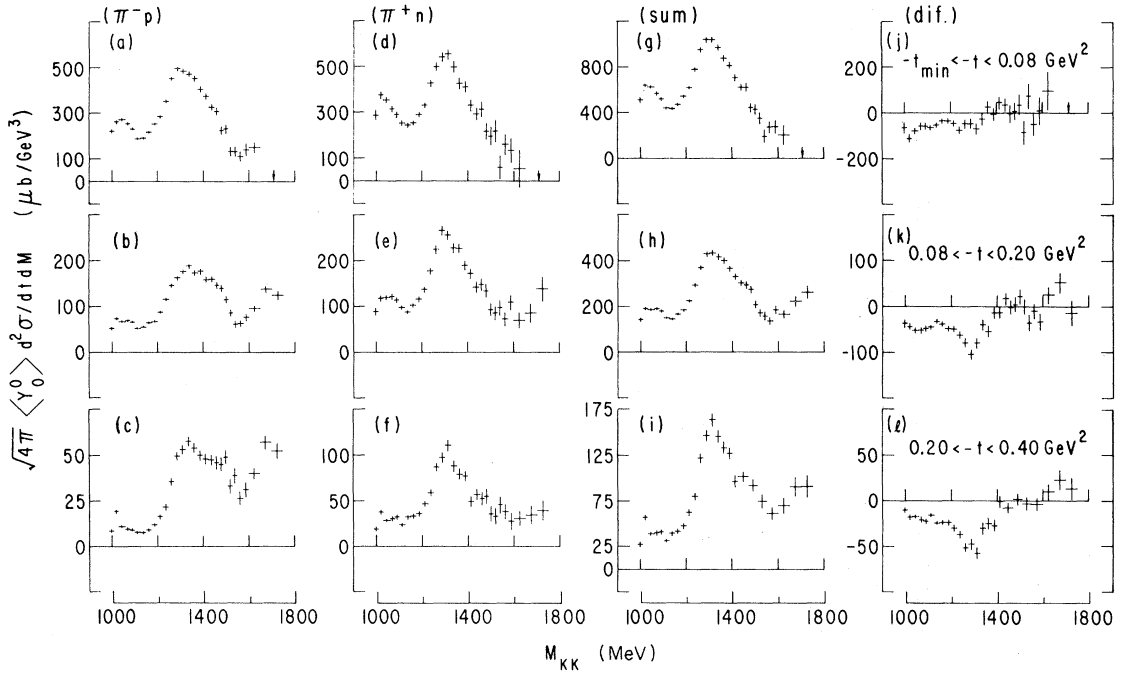

FIG. 4. $\sigma\langle Y_0^0\rangle$ for reactions (1) and (2), their sum and difference, as functions of M for the three t ranges indicated. For $-t < 0.08$ GeV^2, the arrow at 1690 MeV indicates the point at which $t_{min} = -0.08$ GeV^2. The moments are calculated in the t-channel (Jackson) frame.

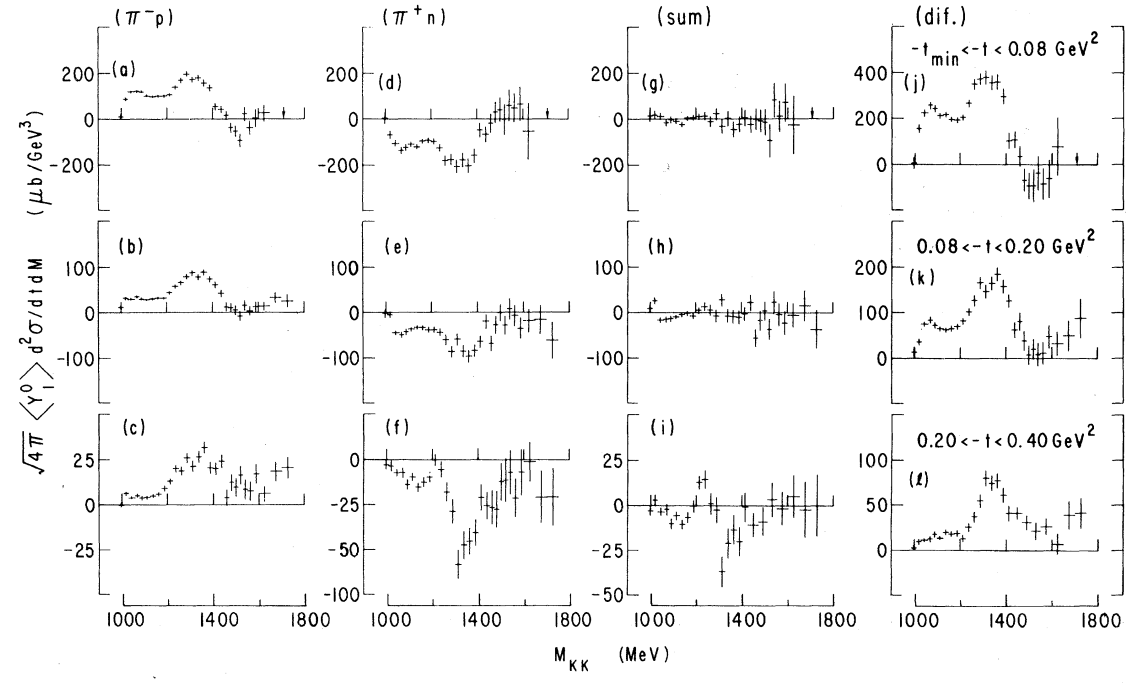

FIG. 5. $\sigma\langle Y_1^0\rangle$ vs M.

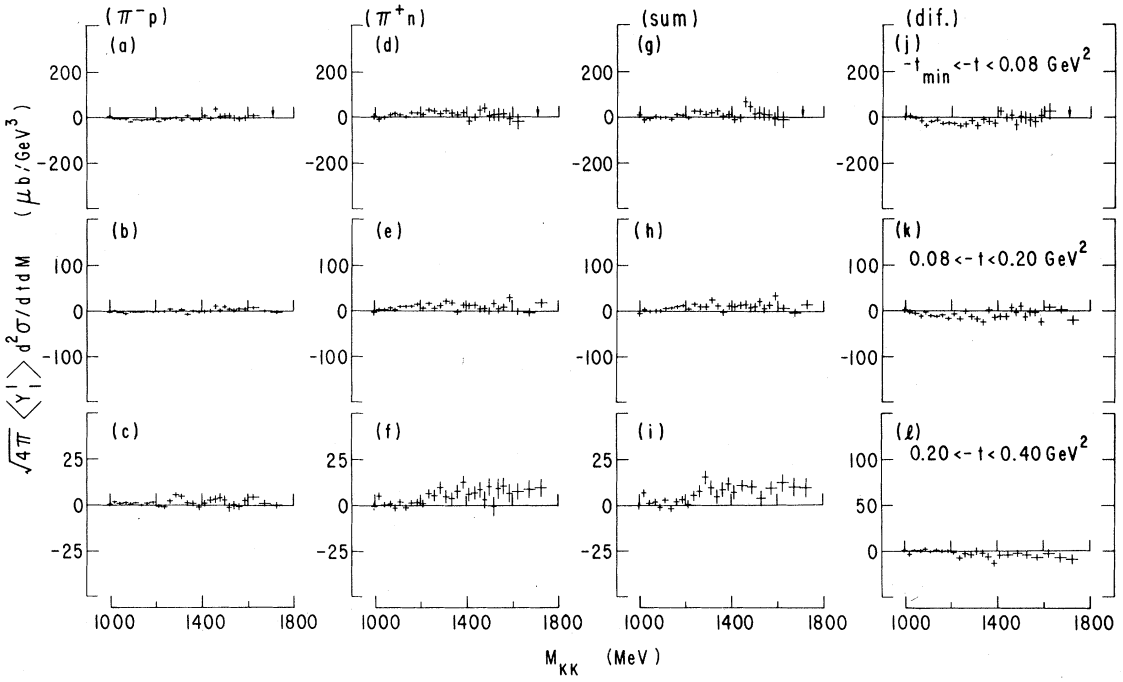

FIG. 6. $\sigma\langle Y_1^1\rangle$ vs M.

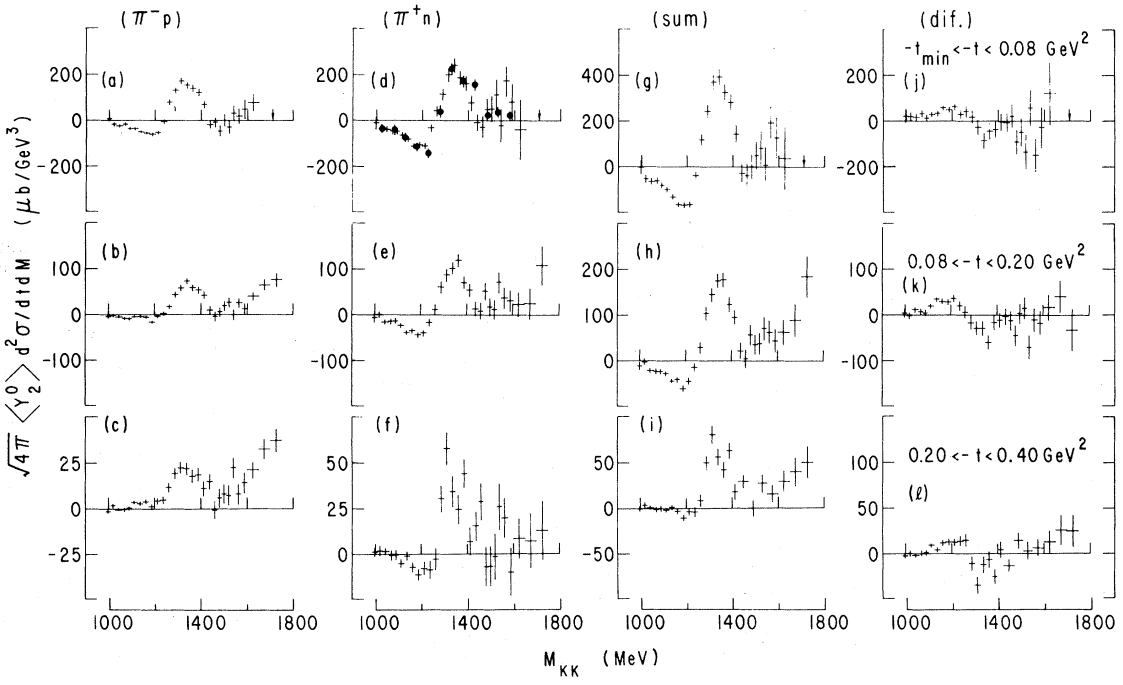

FIG. 7. $\sigma\langle Y_2^0\rangle$ vs M. The solid points in (d) are the $\sigma\langle Y_2^0\rangle$ data of Cason *et al.* (Ref. 5) for reaction (3) for the interval $-t < 0.2$ GeV^2, renormalized so that $\sigma\langle Y_4^0\rangle$ for $1250 < M < 1400$ MeV agrees with $\sigma^+\langle Y_4^0\rangle$ for $-t < 0.08$ GeV^2.

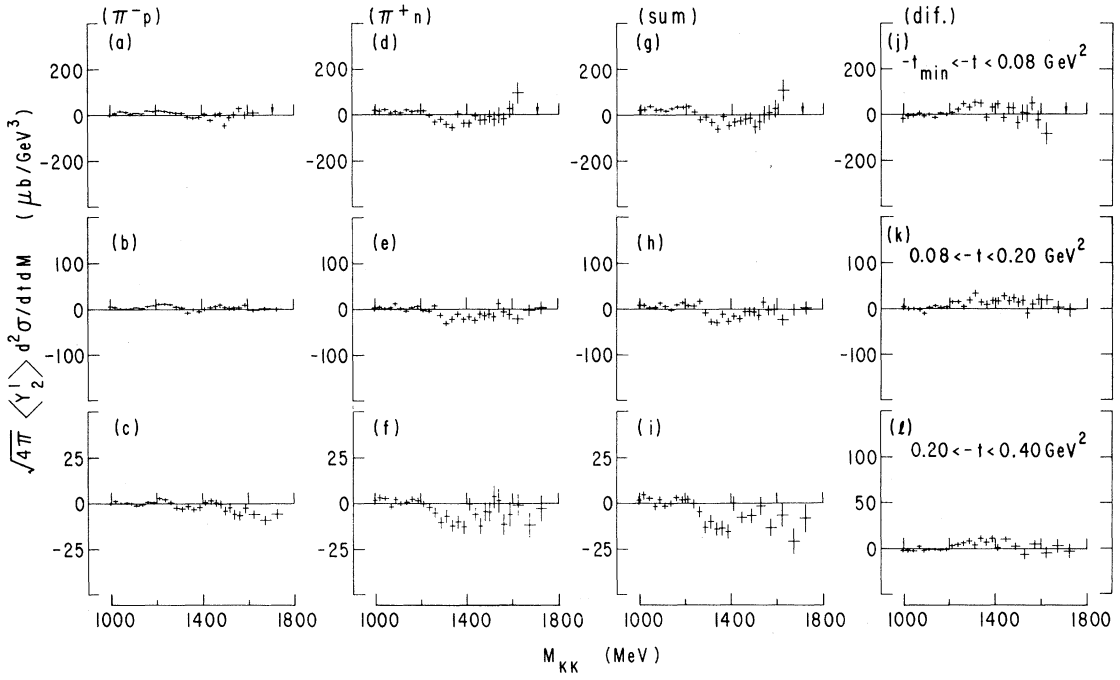

FIG. 8. $\sigma\langle Y_2^1\rangle$ vs M.

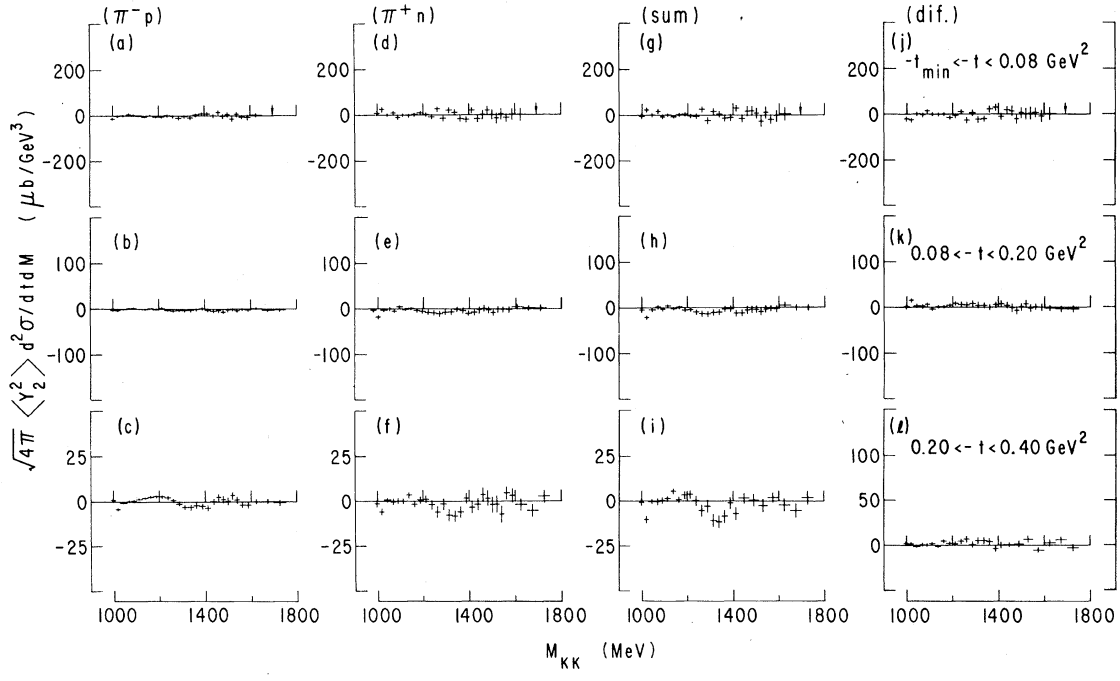

FIG. 9. $\sigma\langle Y_2^2\rangle$ vs M.

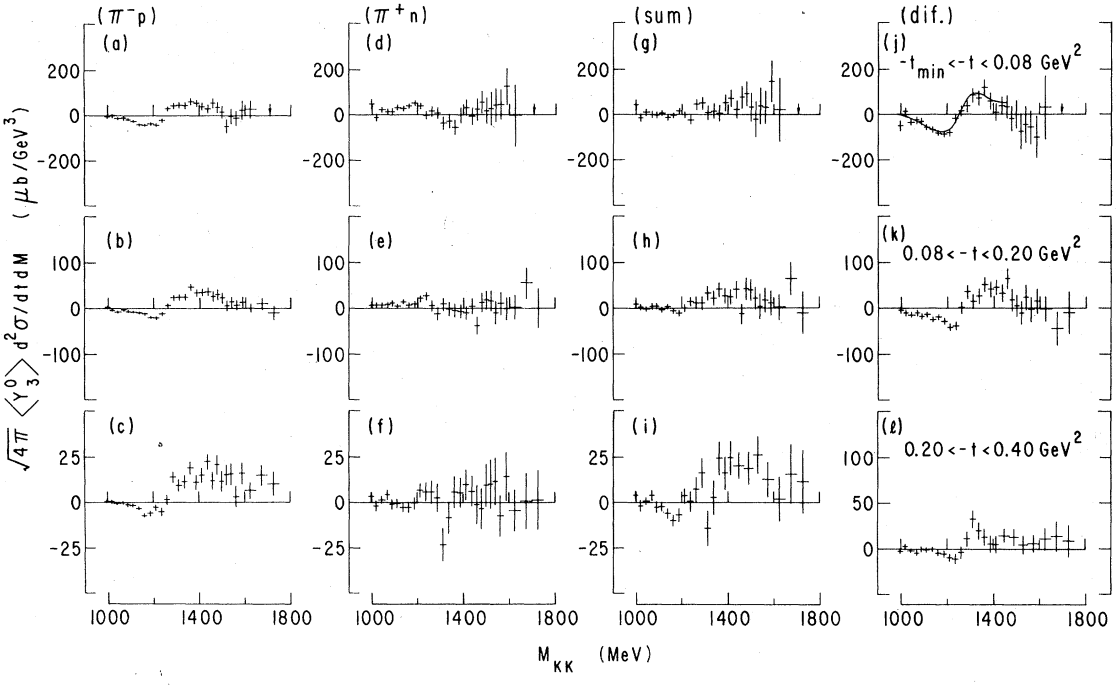

FIG. 10. $\sigma\langle Y_3^0\rangle$ vs M. The curve in (j) is the result of the ρ-f interference fit described in the text.

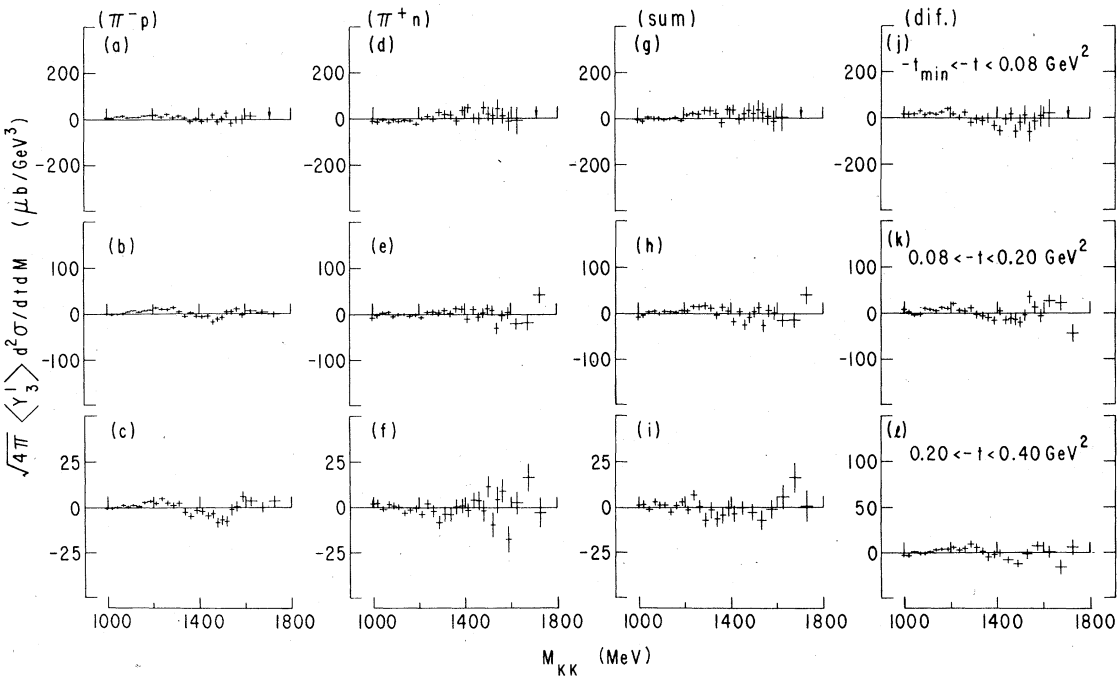

FIG. 11. $\sigma\langle Y_3^1\rangle$ vs M.

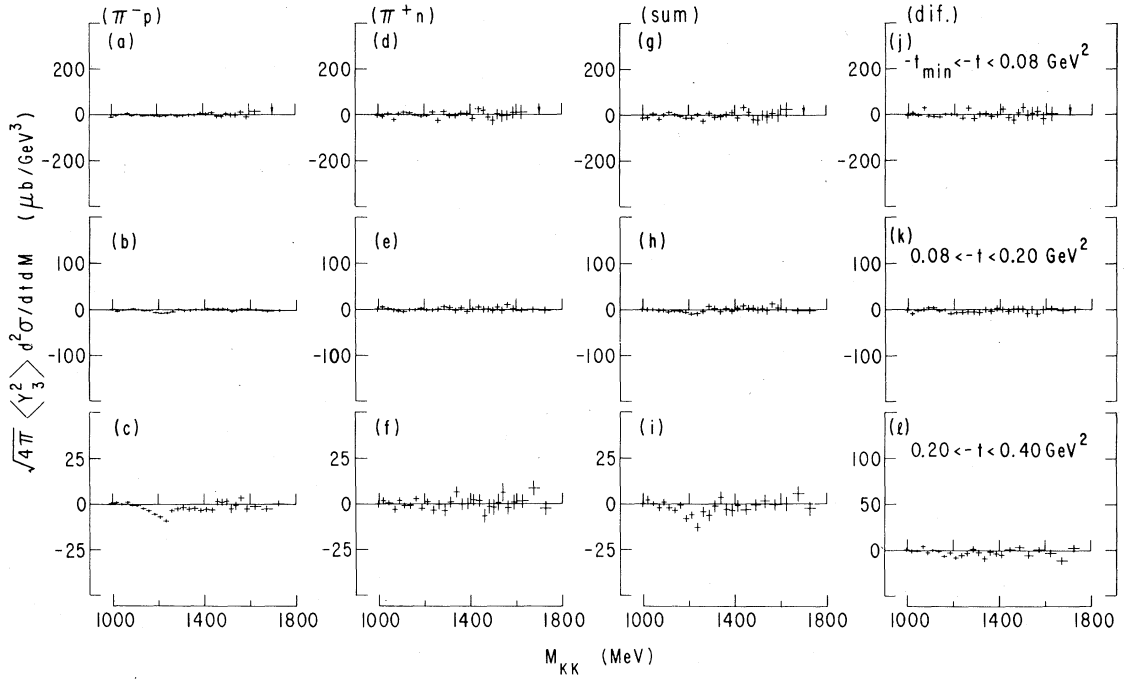

FIG. 12. $\sigma\langle Y_3^2\rangle$ vs M.

The slopes $B_4^{\pm}$ of the $\sigma^{\pm}\langle Y_4^0\rangle t$ distributions are both consistent with the OPE slope of ~12 GeV^{-2} in the $1200<M<1400$ MeV region, where the f meson dominates the D waves. In the range $1450<M<1500$ MeV, f'-A_2^0 interference, which is constructive in reaction (1), causes $B_4^-<B_4^+$.

The slope B_0^+ of $\sigma^+\langle Y_0^0\rangle$ is consistently less than B_0^- for $M\lesssim 1400$ MeV. Since the D-wave contributions have the same slopes in this region ($B_4^-\approx B_4^+$), and since the P wave is small, S-wave interference must be the main cause for the difference in slopes, $B_0^+<B_0^-$, over the entire range from threshold to 1400 MeV.

Because the spin of resonances on the leading meson trajectories increases with mass, the high-order moments become important only at higher masses. Centrifugal-barrier effects (discussed in Sec. IV B) also suppress high-spin effects at

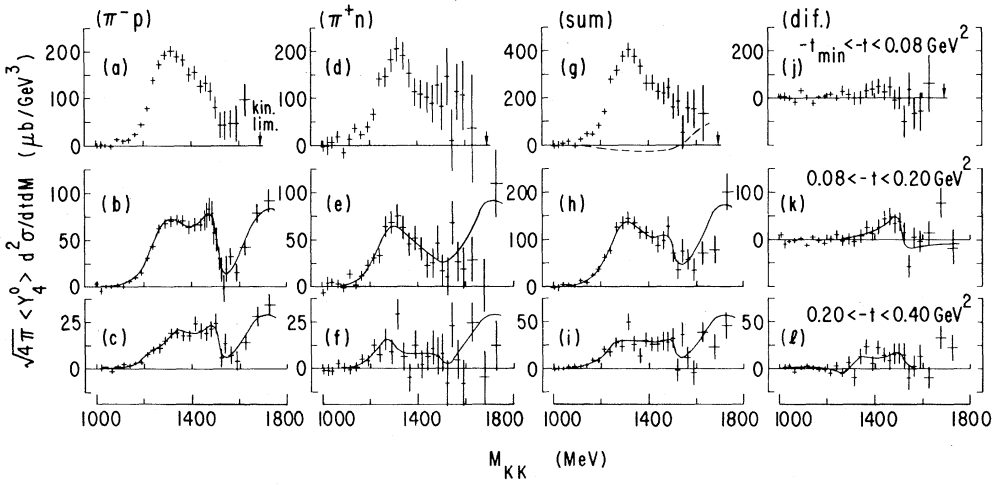

FIG. 13. $\sigma\langle Y_4^0\rangle$ vs M. The solid curves result from the fits described in the text and in Table III. The curve in (g) gives the estimated P-F interference contribution discussed in Ref. 29.

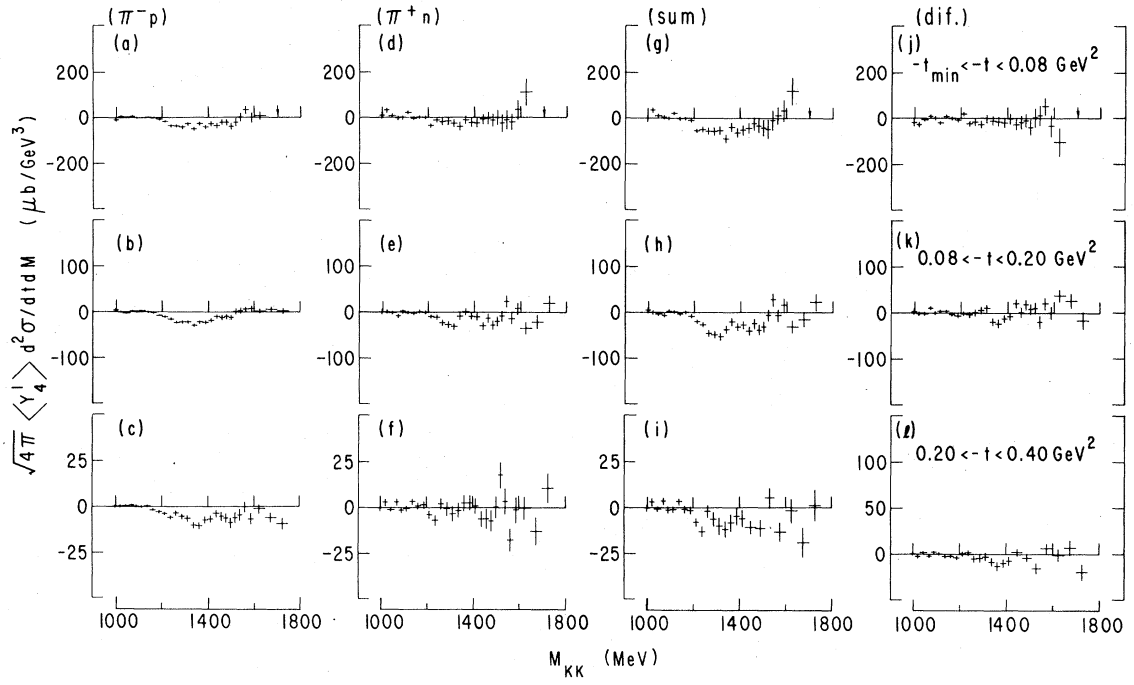

FIG. 14. $\sigma\langle Y_4^1\rangle$ vs M.

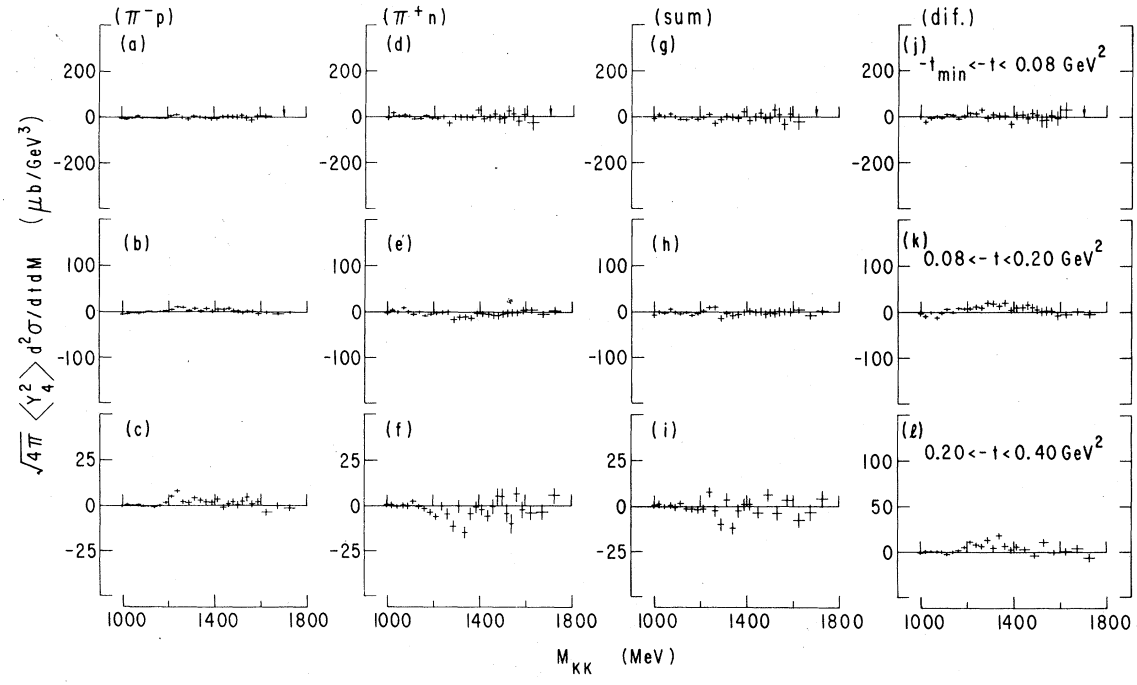

FIG. 15. $\sigma\langle Y_4^2\rangle$ vs M.

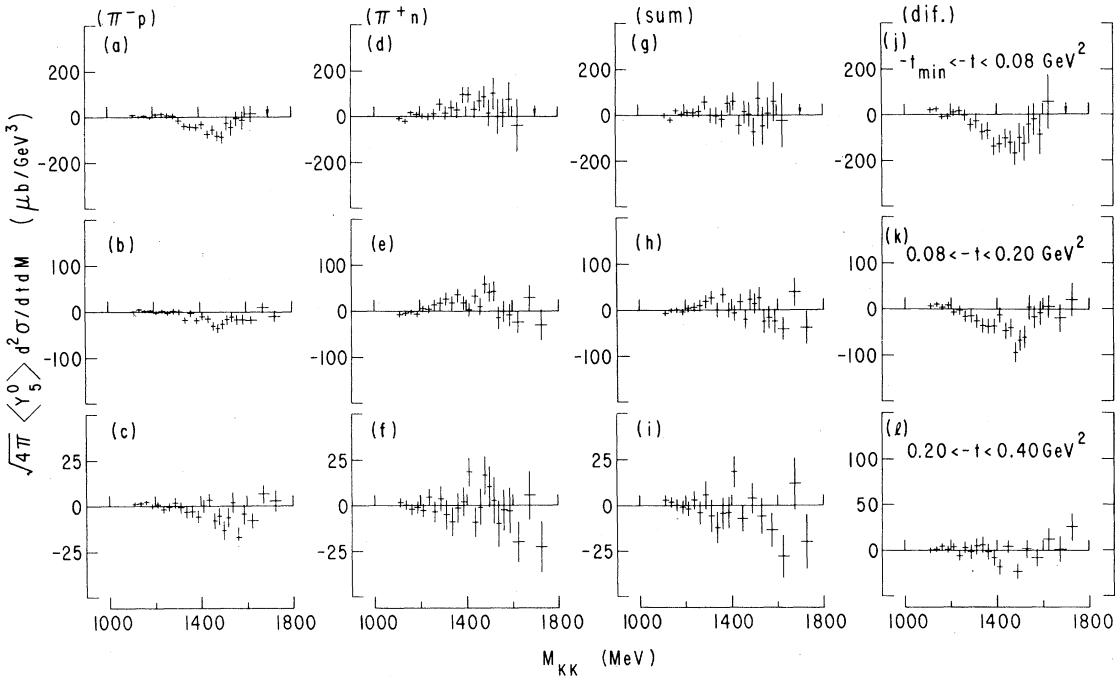

FIG 16. $\sigma\langle Y_5^0\rangle$ vs M.

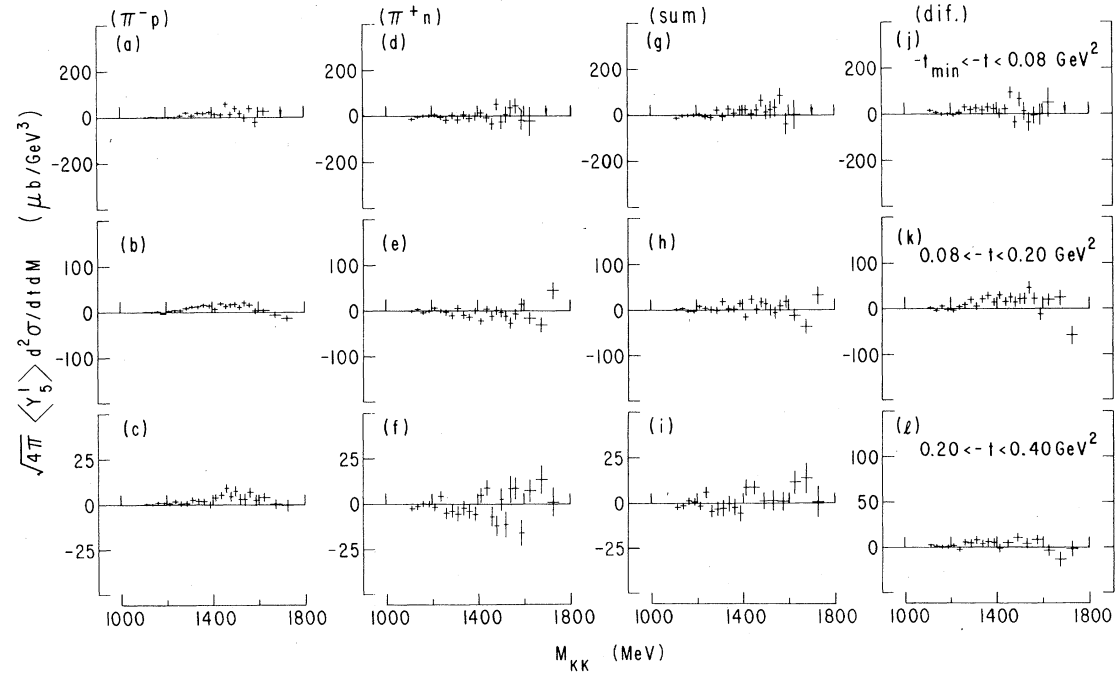

FIG 17. $\sigma\langle Y_5^1\rangle$ vs M.

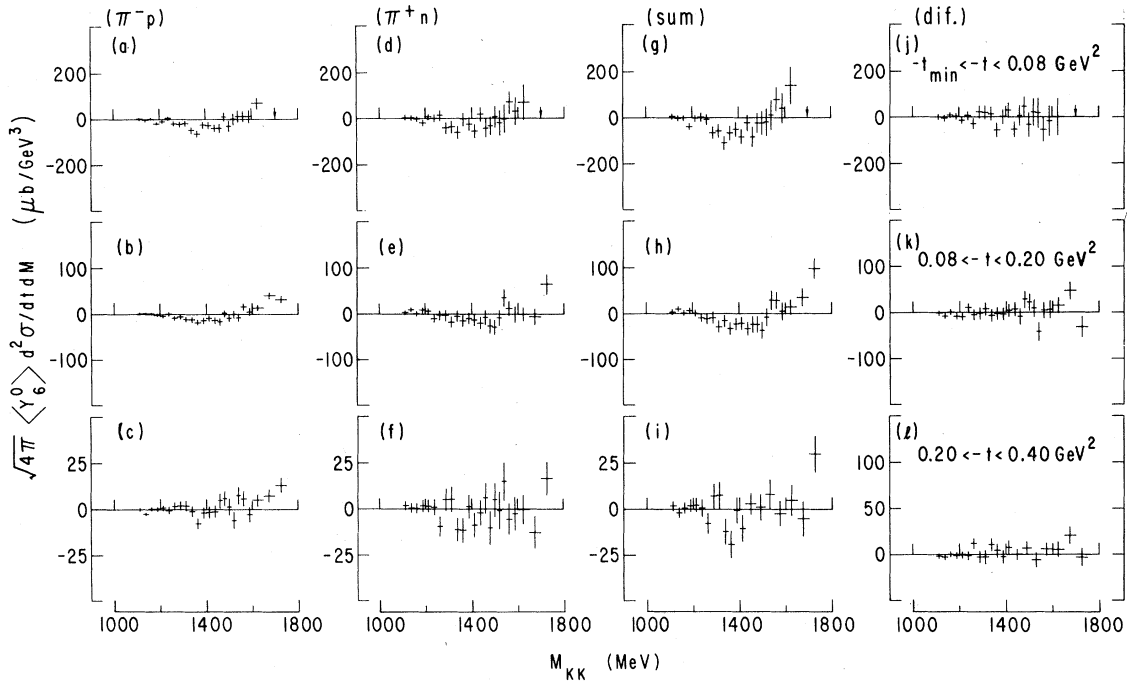

FIG. 18. $\sigma\langle Y_6^0\rangle$ vs M.

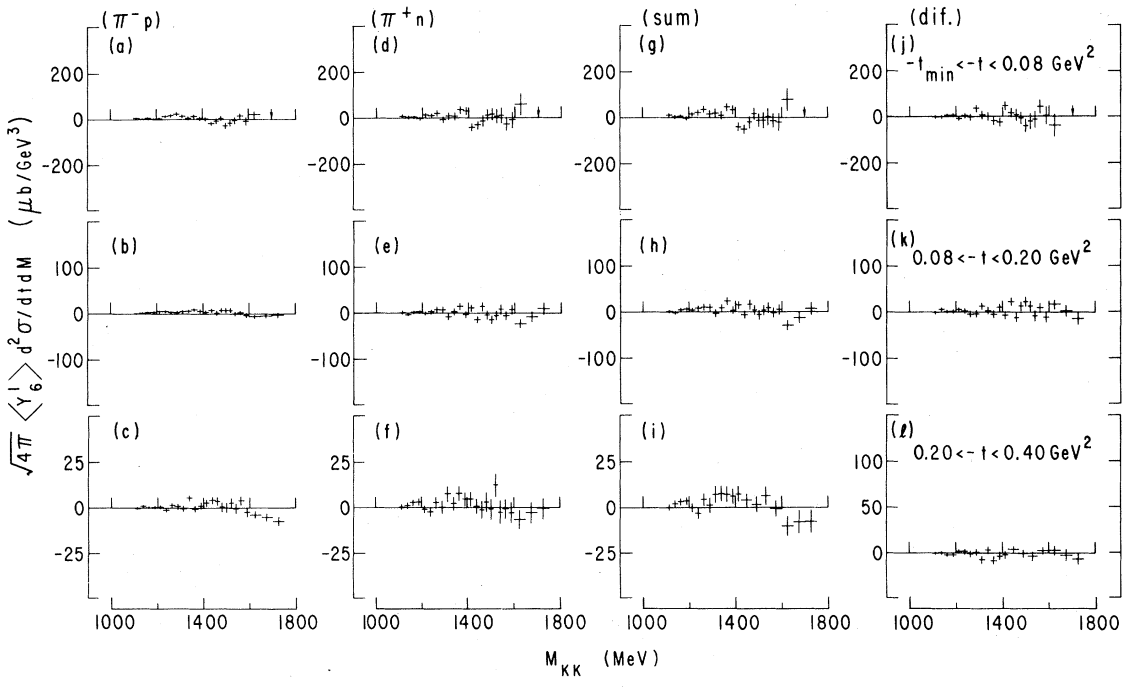

FIG. 19. $\sigma\langle Y_6^1\rangle$ vs M.

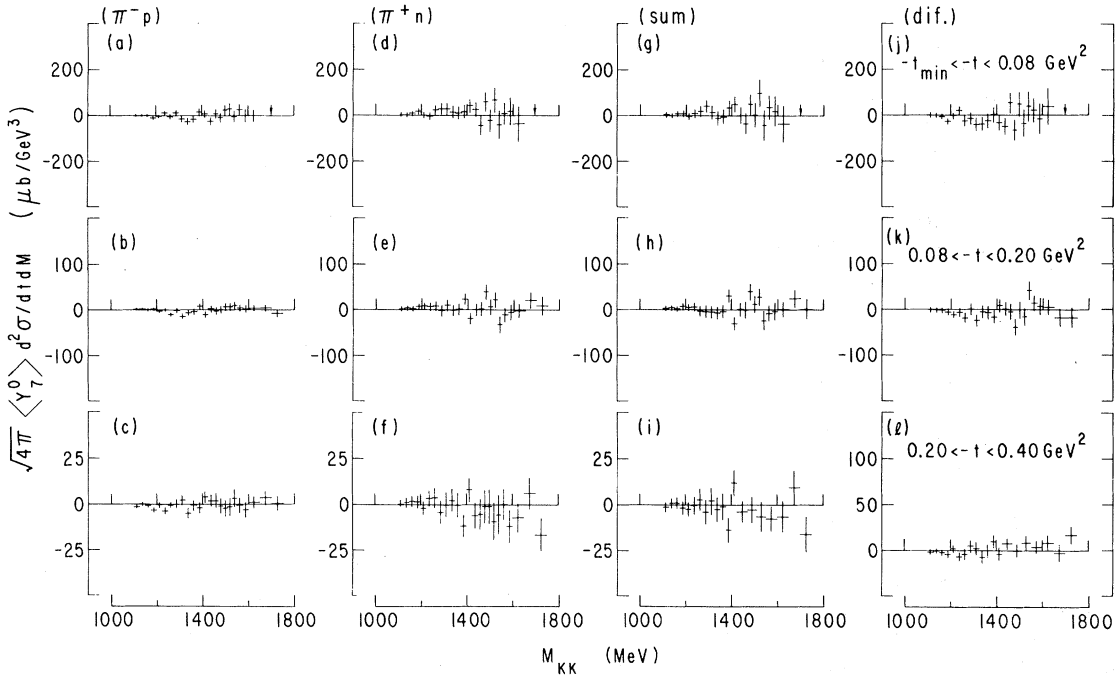

FIG. 20. $\sigma\langle Y_7^0\rangle$ vs M.

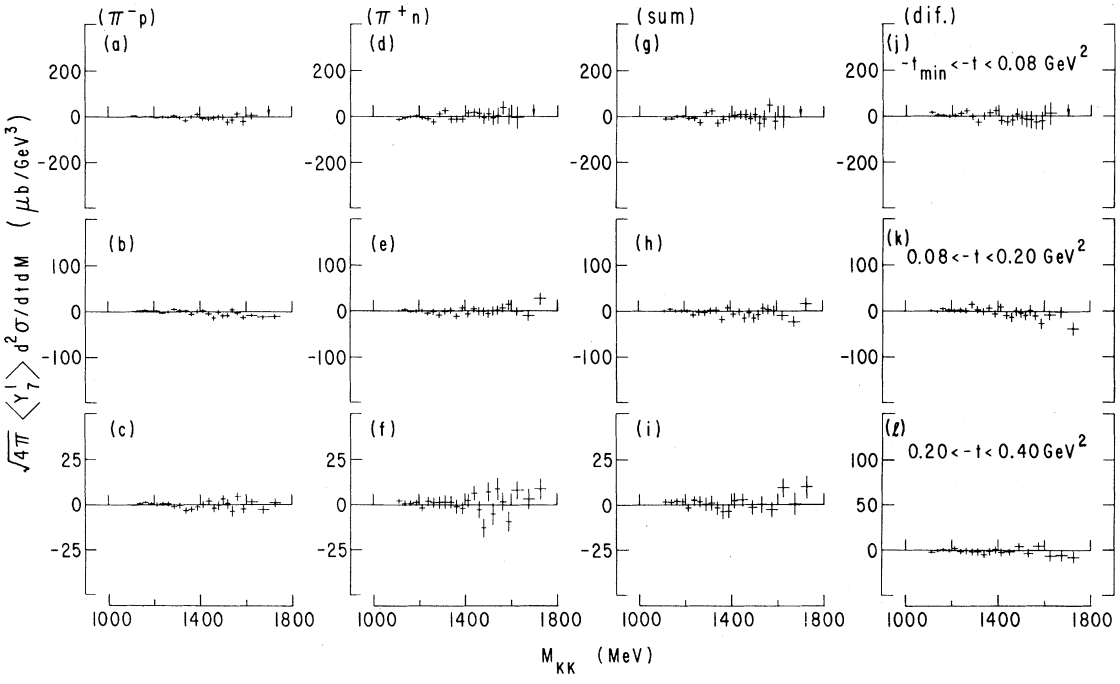

FIG. 21. $\sigma\langle Y_7^1\rangle$ vs M.

TABLE I. Slopes B_L^i from fits of the form $\sigma^i\langle Y_L^0\rangle = A_L^i e^{B_L^i t}$, where $i=-,+$ refers to reactions (1) and (2). $L=0$ or 4 refers to the cross section or Y_4^0 moment. Note that the mass range containing the ϕ meson ($1010 < M < 1030$ MeV) has been omitted.

M (MeV)	$-t$ (GeV^2)	B_0^- (GeV^{-2})	B_0^+ (GeV^{-2})	B_4^- (GeV^{-2})	B_4^+ (GeV^{-2})
988–1010	0.020–0.20	16.2±0.8	10.8±1.3	...	...
1030–1060	0.020–0.20	15.9±0.4	11.9±0.6	...	...
1060–1100	0.020–0.20	14.3±0.3	10.6±0.5	...	...
1100–1150	0.012–0.20	14.2±0.3	10.9±0.5	...	...
1150–1200	0.014–0.20	14.6±0.3	10.3±0.5	...	...
1200–1250	0.020–0.20	13.7±0.3	9.8±0.4	11.7±0.9	11.5±2.0
1250–1300	0.022–0.20	13.1±0.3	8.3±0.4	12.8±0.8	9.5±1.7
1300–1350	0.026–0.20	11.3±0.3	8.7±0.5	11.6±0.9	11.7±1.9
1350–1400	0.030–0.20	10.7±0.3	7.7±0.6	10.5±1.1	9.3±2.7
1400–1450	0.034–0.20	9.8±0.4	9.1±0.9	9.0±1.3	14.1±4.7
1450–1500	0.042–0.20	8.0±0.6	7.5±1.2	4.7±1.4	15.1±6.0

low mass. But at high masses the spectrometer acceptance deteriorates, causing both poor statistics and potential systematic bias in extraction of high-order moments. Constraining the $l \geq 6$ moments to be consistent with zero below 1600 MeV had negligible effect on the moments, so the analysis in Sec. IV is unaffected by the treatment of the high-order moments.

IV. DISCUSSION

As mentioned above, the gross features of our small-t data are as expected for one-pion exchange, and are similar to those seen in $\pi^- p \to \pi^-\pi^+ n$. The $\pi^-\pi^+ n$ data have been interpreted[8,9,26] as production via large nucleon-helicity flip, $m=0$, pion exchange amplitudes L_0^{flip} (where $L=S, P, D, F, G, \ldots$ for $\pi^-\pi^+$ systems of spins 0, 1, 2, 3, 4, ...). Small $m=1$ amplitudes occur, of approximately equal magnitude for both natural- and unnatural-parity exchange. These are L_+ and L_-, respectively, with L_- being dominantly L_-^{flip} from a π-exchange cut contribution, 180° out of phase with L_0^{flip}. In this manner, for example, we have $\sigma\langle Y_{2L}^0\rangle \propto |L_0^{\text{flip}}|^2$ large and positive, $\sigma\langle Y_{2L}^1\rangle \propto \text{Re}(L_0^{\text{flip}} L_-^{\text{flip}*})$ small and negative, approximately a reduced-magnitude mirror image of $\sigma\langle Y_{2L}^0\rangle$, while $\sigma\langle Y_{2L}^2\rangle \propto |L_-|^2 - |L_+|^2 \approx 0$. In Table II we list the $\sigma\langle Y_l^m\rangle$ for $l \leq 6$ and $m \leq 2$ in terms of contributions from amplitudes with spin $L \leq 3$ and $m \leq 1$, as well as the $\sigma\langle Y_7^m\rangle$ in terms of F-G interferences. Note that the identification of the amplitudes with definite natural- or unnatural-parity exchange is exact only asymptotically as $s \to \infty$.

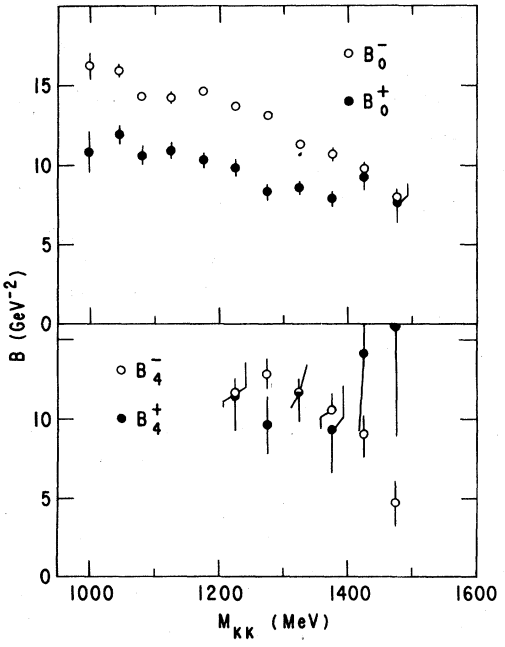

FIG. 22. Slopes $B_L^{\mp}$ of t distributions of $\sigma^{\mp}\langle Y_L^0\rangle$ as functions of M for reactions (1) and (2); the slopes are those given by the exponential fits (over the range $-t < 0.20$ GeV^2) shown in Table I.

In this section, we will not attempt an amplitude analysis, but will confine our discussion to those features of the data which can be directly interpreted. Since, at a given mass, the effects of the highest-spin amplitude that is significantly present are the most obvious and interpretable (see Table II), we will begin our discussion in Sec. IV A with an analysis of the Y_4^0 moment, where we study the D-wave amplitudes. We then consider the P waves in Sec. IV B and the S waves in Sec. IV C.

A. D-wave effects

We have studied[10] the tensor mesons in reactions (1) and (2) by means of the Y_4^0 moment, which is dominated by the f meson for $M < 1500$ MeV and $-t \lesssim 0.20$ GeV^2. There are in general 10 D-wave amplitudes for each of the produced tensor mesons: five meson helicity states (m)

TABLE II. The moments $\sigma\langle Y_l^m\rangle$ in terms of the amplitudes L_0, L_-, and L_+ defined in the text. In these expressions, we use the convention that $AB \equiv \mathrm{Re}(AB^*)$ and an implicit summation over nucleon helicity indices is implied: $AB \equiv \mathrm{Re}(A^{\mathrm{flip}}B^{\mathrm{flip}*}) + \mathrm{Re}(A^{\mathrm{nonflip}}B^{\mathrm{nonflip}*})$. We also use the convention $A^2 \equiv |A|^2 = |A^{\mathrm{flip}}|^2 + |A^{\mathrm{nonflip}}|^2$.

$$\sigma\langle Y_0^0\rangle = S_0^2 + P_0^2 + P_-^2 + P_+^2 + D_0^2 + D_-^2 + D_+^2 + F_0^2 + F_-^2 + F_+^2$$

$$\sigma\langle Y_1^0\rangle = 2S_0P_0 + 1.789P_0D_0 + 1.549(P_-D_- + P_+D_+) + 1.757D_0F_0 + 1.656(D_-F_- + D_+F_+)$$

$$\sigma\langle Y_1^1\rangle = 1.414S_0P_- + 1.096P_0D_- - 0.633P_-D_0 - 1.014D_0F_- - 1.434D_-F_0$$

$$\sigma\langle Y_2^0\rangle = 0.894P_0^2 - 0.447(P_-^2 + P_+^2) + 0.639D_0^2 + 0.319(D_-^2 + D_+^2) + 0.596F_0^2 + 0.447(F_-^2 + F_+^2) + 2S_0D_0 + 1.757P_0F_0 + 1.434(P_-F_- + P_+F_+)$$

$$\sigma\langle Y_2^1\rangle = 1.414S_0D_- + 1.096P_0P_- + 1.171P_0F_- - 0.717P_-F_0 + 0.452D_0D_- + 0.298F_0F_-$$

$$\sigma\langle Y_2^2\rangle = 0.548(P_-^2 - P_+^2) + 0.391(D_-^2 - D_+^2) + 0.365(F_-^2 - F_+^2) - 0.293(P_-F_- - P_+F_+)$$

$$\sigma\langle Y_3^0\rangle = 2S_0F_0 + 1.757P_0D_0 - 1.014(P_-D_- + P_+D_+) + 1.193D_0F_0 + 0.422(D_-F_- + D_+F_+)$$

$$\sigma\langle Y_3^1\rangle = 1.414S_0F_- + 1.171P_0D_- + 1.014P_-D_0 + 0.633D_0F_- + 0.298D_-F_0$$

$$\sigma\langle Y_3^2\rangle = 0.926(P_-D_- - P_+D_+) + 0.578(D_-F_- - D_+F_+)$$

$$\sigma\langle Y_4^0\rangle = 1.746P_0F_0 - 1.069(P_-F_- + P_+F_+) + 0.857D_0^2 - 0.571(D_-^2 + D_+^2) + 0.601F_0^2 + 0.091(F_-^2 + F_+^2)$$

$$\sigma\langle Y_4^1\rangle = 0.414P_0F_- + 0.976P_-F_0 + 1.107D_0D_- + 0.498F_0F_-$$

$$\sigma\langle Y_4^2\rangle = 0.845(F_-P_- - F_+P_+) + 0.452(D_-^2 - D_+^2) + 0.288(F_-^2 - F_+^2)$$

$$\sigma\langle Y_5^0\rangle = 1.699D_0F_0 - 1.201(D_-F_- + D_+F_+)$$

$$\sigma\langle Y_5^1\rangle = 1.140D_0F_- + 1.075D_-F_0$$

$$\sigma\langle Y_5^2\rangle = 0.871(D_-F_- - D_+F_+)$$

$$\sigma\langle Y_6^0\rangle = 0.840F_0^2 - 0.630(F_-^2 + F_+^2)$$

$$\sigma\langle Y_6^1\rangle = 1.112F_0F_-$$

$$\sigma\langle Y_6^2\rangle = 0.431(F_-^2 - F_+^2)$$

$$\sigma\langle Y_7^0\rangle = 1.672F_0G_0 - 1.295(F_-G_- + F_+G_+)$$

$$\sigma\langle Y_7^1\rangle = 1.131F_0G_- + 1.095F_-G_0$$

$$\sigma\langle Y_7^2\rangle = 0.848(F_-G_- - F_+G_+)$$

for each of two nucleon helicity states (λ). Of the f, f', and A_2^0, only the f meson's production mechanisms are currently well understood[8,9] (pion exchange dominates at small t), so an analysis allowing for the effects of all 10 amplitudes is needed. To the extent that the mass dependence is the same for each of the 10 amplitudes for a given resonance (each of the 10 of course having its own overall magnitude and production phase), we can exploit the mass dependence to extract from the Y_4^0 moment the contributions from each resonance and the several interferences among resonances. For the dominant f meson, this is known to be a good approximation, since f production is dominated by a single amplitude, L_0^{flip}, while the small L_-^{flip} amplitude arises from an absorptive cut whose strength is mass-dependent.[8,9] For the f' and A_2^0 no direct information is available on the mass dependence of individual amplitudes. In what follows, we assume that all significant amplitudes for a given resonance have the same mass dependence, namely, the D-wave Breit-Wigner decay amplitude $B_i(M)$ (Ref. 27) for the ith tensor meson, while the production amplitude $A_i^{\lambda m}(t)$ contains the t dependence.[28] Then the total amplitude for production of a K^-K^+n final state (λ, m) is $D^{\lambda m}(M,t) = \sum A_i^{\lambda m}(t)B_i(M)$. The most general contribution of the three tensor mesons to $\sigma^-\langle Y_4^0\rangle$ is

$$\sigma^-\langle Y_4^0\rangle = \sum Q_k(t)\,F_k(M)\,. \tag{5}$$

The nine mass functions $F_k(M)$ are given in Table III and are shown in Fig. 23; the $Q_k(t)$ functions are linear combinations of terms of the form $\mathrm{Re}[A_i^{\lambda m}(t)A_j^{\lambda m}(t)^*]$ or $\mathrm{Im}[A_i^{\lambda m}(t)A_j^{\lambda m}(t)^*]$.

With the addition to Eq. (5) of a 10th term, for the g-meson contribution at high masses, we can fit[29] $\sigma^-\langle Y_4^0\rangle$ (and simultaneously $\sigma^+\langle Y_4^0\rangle$, with sign changes of appropriate Q_k) for masses $M < 1750$ MeV. The results of fits to our data, shown as functions of M in broad t bands, are given in Table III and are shown in Fig. 13. Each t interval was fitted independently, with $\sigma^-\langle Y_4^0\rangle$ and $\sigma^+\langle Y_4^0\rangle$ being fitted simultaneously using 12 free

TABLE III. Parameters determined from the fits described in the text. B_g is a Breit-Wigner form for spin 3 ($M_g = 1713$ MeV, $\Gamma_g = 228$ MeV). [Note that the factors $2M$ in the $F_k(M)$ convert from $d^2\sigma/dtdM^2$ to $d^2\sigma/dtdM$; see, e.g., Appendix A of Ref. 28.] The error on a given parameter corresponds to the change which increases χ^2 by 1 when the remaining 11 parameters are reoptimized.

	Q_k (μb/GeV)	
	$-t$ range 0.08–0.20 GeV^2	$-t$ range 0.20–0.40 GeV^2
$F_k(M)/2M$		
$\lvert B_f\rvert^2$	4.02 ± 0.14	1.04 ± 0.06
$\lvert B_{f'}\rvert^2$	0.08 ± 0.08	−0.06 ± 0.03
$\lvert B_A\rvert^2$	0.04 ± 0.07	−0.08 ± 0.03
$\mathrm{Re}(B_f B_{f'}^*)$	−1.40 ± 0.25	−0.08 ± 0.13
$\mathrm{Re}(B_f B_A^*)$	−0.39 ± 0.15	0.18 ± 0.06
$\mathrm{Re}(B_{f'} B_A^*)$	−0.59 ± 0.22	−0.09 ± 0.12
$\mathrm{Im}(B_f B_{f'}^*)$	0.24 ± 0.21	0.48 ± 0.16
$\mathrm{Im}(B_f B_A^*)$	0.43 ± 0.20	−0.36 ± 0.14
$\mathrm{Im}(B_{f'} B_A^*)$	−1.00 ± 0.30	−0.21 ± 0.07
$\lvert B_g\rvert^2$	6.68 ± 1.20	2.23 ± 0.38
$M_{f'}$ (MeV)	1506 ± 6	1510 ± 13
$\Gamma_{f'}$ (MeV)	70 ± 12	55 ± 19
χ^2/DF	49.1/44	52.4/44

parameters: the coefficients of the nine D-wave terms, the g-meson term, and the f' mass and width. Figure 24 shows the individual contributions to $\sigma_{\mathrm{sum}}\langle Y_4^0\rangle$ and $\sigma_{\mathrm{dif}}\langle Y_4^0\rangle$ for $0.08 < -t < 0.20$ GeV^2. For the interference terms the notation is such that, e.g., fA_2 is the sum of the $\mathrm{Re}(B_f B_A^*)$ and $\mathrm{Im}(B_f B_A^*)$ terms (multiplied by 2 since sum and difference get equal-sized terms from each of σ^- and σ^+). A number of conclusions can be drawn.

$f \to \bar{K}K$ branching ratio. We have calculated the $f \to \bar{K}K$ branching ratio by comparing $Q_f(K^-K^+)$, the coefficient of $\lvert B_f\rvert^2$ in the fits to $\sigma^{\mp}\langle Y_4^0\rangle$, to $Q_f(\pi^-\pi^+)$, the analogous coefficient from a fit to our $\pi^- p \to \pi^-\pi^+ n$ data from an earlier experiment[20]; the $\pi^-\pi^+$ experiment was performed with the same apparatus and at the same beam momentum. Both the $\pi^-\pi^+$ and K^-K^+ data were fitted in the range $0.08 < -t < 0.40$ GeV^2; terms in Eq. (5) involving f' or A_2^0 were set equal to zero in fitting the $\pi^-\pi^+$ data. $\sigma\langle Y_4^0\rangle$ for the $\pi^-\pi^+$ data, along with the fitted curve, is shown in Fig. 25. After including a ±10% relative normalization uncertainty between the $\pi^-\pi^+$ and K^-K^+ experiments, we found $(f \to K^-K^+/f \to \pi^-\pi^+) = (3.5 \pm 0.4)\%$, leading to $(f \to \bar{K}K/f \to \mathrm{all}) = (3.8 \pm 0.4)\%$, where we have used[13] $(f \to \pi\pi/f \to \mathrm{all}) = 0.81 \pm 0.01$ and the isospin relations for the $I = 0$ f meson, $K^-K^+/\bar{K}K = \frac{1}{2}$ *and* $\pi^-\pi^+/\pi\pi = \frac{2}{3}$. This is the first determination of the $f \to \bar{K}K$ branching ratio which has quantitatively accounted for both f' and A_2^0 effects and used K^-K^+ and $\pi^-\pi^+$ data taken with the same apparatus at the same beam momentum. The analyses had many elements in common, minimizing various potential systematic errors (such as overall normalization) in this measurement of the

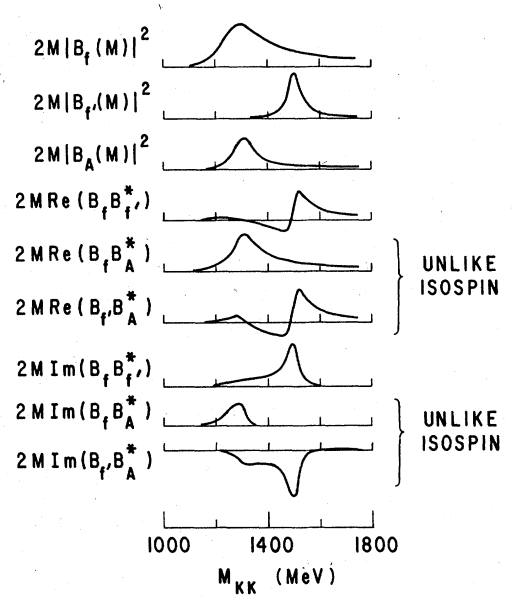

FIG. 23. The mass functions defined in Table III and Eq. (5). The vertical scales are arbitrary.

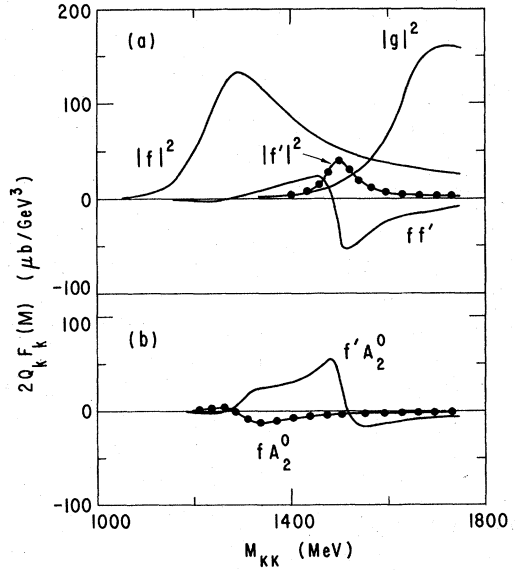

FIG. 24. The contributions to (a) $\sigma_{\mathrm{sum}}\langle Y_4^0\rangle$ and (b) $\sigma_{\mathrm{dif}}\langle Y_4^0\rangle$ for $0.08 < -t < 0.20$ GeV^2, resulting from the fit described in the text. The $|A_2^0|^2$ contribution to the fit is negligibly small and is not displayed.

branching ratio. Our result for $(f \to \bar{K}K/f \to \text{all})$ can be compared with the SU(3) prediction[30] of 3.3%, the world average[13] of $(2.7 \pm 0.6)\%$, and a recent determination by Wetzel *et al.*[4] of $(2.4 \pm 0.5)\%$. This latter determination was based on an analysis of the reaction $\pi^- p \to K_S^0 K_S^0 n$ at 8.9 GeV/c; the values for $\sigma\langle Y_4^0\rangle$ from that experiment agree extremely well with our values for $\sigma^+\langle Y_4^0\rangle$ in the f mass region (after correcting for the $K_L^0 K_L^0 n$ final state and the measured energy dependence[4] of p_{lab}^{-2}). The difference between their branching ratio and our result may be related to the fact that their determination relied on a one-pion exchange model with absorption, rather than a direct comparison with $f \to \pi^-\pi^+$.

f-A_2^0 interference. This term is sizable only for $-t > 0.20$ GeV^2. The f-A_2^0 relative production phase of $(63^{+11}_{-15})^\circ$ implied by the fit for $-t > 0.20$ GeV^2 agrees with the prediction by Irving and Michael[28] of $\sim 70^\circ$; their prediction is based on model amplitudes derived from duality and vector-meson production studies. For $-t < 0.20$ GeV^2, this term is much less important than f'-A_2^0 interference, despite the dominance of the f in the total cross section; therefore f' and A_2^0 production must have important contributions that are coherent with one another but which are incoherent with the f, i.e., production amplitudes (λ, m) different from those responsible for f production. This is consistent with a model[28,31] in which small-t A_2^0 production is dominated by nucleon-helicity-nonflip $Z(J^{PC}=2^{--})$ exchange, giving an amplitude D_0^{nonflip} incoherent with dominant D_0^{flip} OPE amplitude of the f. At larger t, B exchange becomes an important mechanism for A_2^0 production, contributing to D_0^{flip}, so f-A_2^0 interference becomes detectable. From Ref. 28, we expect $|fA_2^{0*}|/|f|^2$ to be 2 to 3 times larger at $-t \sim 0.3$ GeV^2 than at $-t \sim 0.1$ GeV^2, consistent with our observation.

To get a feeling for the relative amount of small-t A_2^0 production by the D_0^{flip} amplitude, we have extrapolated (as p_{lab}^{-2}) the 4-GeV/c $\pi^+ n \to A_2^0 p$ data of Emms *et al.*,[32] who determined $|D_0|^2 = |D_0^{\text{flip}}|^2 + |D_0^{\text{nonflip}}|^2$. For $0.08 < -t < 0.20$ GeV^2, an f-A_2^0 contribution to $\sigma^-\langle Y_4^0\rangle$ of 39 ± 15 μb GeV^{-3} (averaged over $1300 < M < 1400$ MeV) would be implied if A_2^0 production were purely flip with the phase predicted by Ref. 28. The values given in Table III and displayed in Fig. 24 give a contribution of -5 ± 3 μb GeV^{-3}. Thus, the amount of D_0^{flip} for A_2^0 production may be quite small in the region $-t < 0.20$ GeV^2 compared to D_0^{nonflip}, contrary to the assumption made by Emms *et al.*[32] In the same M and t range, an $|A_2^0|^2$ contribution of ≤ 15 μb GeV^{-3} is expected, compared to the very small value of 0.5 ± 0.9 μb GeV^{-3} found by our fits. This difference may result from the increasing relative importance of natural-parity exchange with energy.

f' mass and width. $\sigma^-\langle Y_4^0\rangle$ exhibits a striking interference pattern near 1500 MeV due to interference of the narrow f' with the slowly varying high-mass tails of the f and A_2^0 Breit-Wigner amplitudes. Our fits, which yield $M_{f'} = 1506 \pm 5$ MeV and $\Gamma_{f'} = 66 \pm 10$ MeV,[33] explicitly take interference effects into account in measuring the f' parameters. The currently accepted values[13] of $M_{f'} = 1516 \pm 3$ MeV and $\Gamma_{f'} = 40 \pm 10$ MeV may be *systematically* in error owing to the neglect of interference effects[34] in previous f' studies using the reactions $\bar{K}N \to \bar{K}K\Lambda, \bar{K}K\Sigma^0$. Table IV shows our results and those of several recent $\bar{K}N \to \bar{K}K\Lambda$, $\bar{K}K\Sigma^0$ experiments,[14,15] as well as the previous world average values.[13] These recent experiments taken together favor a significantly greater width than the most recent Particle Data Group average.[13]

f'-A_2^0 interference. As shown in Fig. 24, f'-A_2^0 interference is as large an effect as f-f' interference in the $-t$ region 0.08 to 0.20 GeV^2. This is somewhat surprising since the $f \to K^-K^+$ cross section in the f' mass region is about 10 times that of the A_2^0. Apparently there is considerable coherence between the f' and A_2^0 amplitudes, in contrast to the small f-A_2^0 coherence.

2^{++} nonet mixing angle and $f' \to \pi\pi$ branching ratio. f-f' interference is significant for $-t < 0.40$ GeV^2. The crudely determined t dependence of $\text{Re}(B_f B_{f'}^*)$ is compatible with an OPE production mechanism (i.e., e^{12t} for $-t \lesssim 0.20$ GeV^2) for that part of the f' amplitude coherent with the f amplitude. In the OPE-dominated range $0.08 < -t < 0.20$ GeV^2, the fit to $\sigma^\mp\langle Y_4^0\rangle$ implies an f-f' relative production phase of $(170 \pm 10)^\circ$, consistent with OPE which allows either 0° or 180°. The 180° value determines[6,35] the 2^{++} nonet mixing angle to be (in the limit that the $\lambda\bar{\lambda}$ content of the f' does not couple to $\pi\pi$) less than the ideal angle of $\arctan(1/\sqrt{2}) = 35.26^\circ$. In the same limit, the value of the $f' \to \pi\pi$ branching ratio found below implies a mixing angle of $(32.5 \pm 0.5)^\circ$, via the relation[36] $\tan^2(\theta - \theta_{\text{ideal}}) = g_{f'\pi\pi}^2/g_{f\pi\pi}^2$. The mass formulas also give values somewhat less than ideal for this mixing angle, $(29 \pm 2)^\circ$ for the linear mass formula and $(31 \pm 2)^\circ$ for the quadratic.[13]

Following arguments given by Beusch *et al.*,[3,4] if the f' were produced only by OPE, then the Breit-Wigner squared terms would be related to the branching ratios by

$$\frac{M_{f'}\, q_\pi(M_f) Q_f\, |B_f(M_f)|^2}{M_f q_\pi(M_{f'}) Q_{f'}\, |B_{f'}(M_{f'})|^2} = \frac{(f \to \bar{K}K/f \to \text{all})(f \to \pi\pi/f \to \text{all})}{(f' \to \bar{K}K/f' \to \text{all})(f' \to \pi\pi/f' \to \text{all})} \,. \quad (6)$$

Equation (6) can be solved for $(f' \to \pi\pi / f' \to \text{all})$; all other quantities are known. We use the $(f \to \bar{K}K / f \to \text{all})$ value determined above, the estimate of $(f \to \bar{K}K / f' \to \text{all}) = 0.70$ of Ref. 30, and the Particle Data Group[13] value of $(f \to \pi\pi / f \to \text{all}) = 0.81 \pm 0.01$. Q_f and $M_{f'}$ are taken from the best fit to the $0.08 < -t < 0.20$-GeV^2 data. $Q_{f'}$ for pure OPE is deduced from Q_f and $Q_{ff'}$ since $Q_{f'}$ from the fit includes non-OPE contributions as noted above. Schematically, $|f'_{\text{OPE}}|^2 = |\text{Re}(ff'^*)/[|f|\cos(\varphi_f - \varphi_{f'})]|^2$. Equation (6) then yields[37] $(f' \to \pi\pi / f' \to \text{all}) = (1.2 \pm 0.4)\%$.

This branching ratio exceeds the upper limit of 0.9% obtained in a similar analysis by Beusch *et al.*[3] of their $\pi^- p \to K_S^0 K_S^0 n$ data at 8.9 GeV/c. Their data are consistent with our results for reaction (2), but the dominant f' effects, namely the f-f' and f'-A_2^0 interferences, tend to cancel one another in these reactions. Our analysis depends on having results from both reactions (1) and (2), so that the f-f' interference term can be separated from the f'-A_2^0 term. The best existing direct measurements of $f' \to \pi\pi$ yielded upper limits of 6% (90% CL) (Ref. 14) from a comparison of $\pi^-\pi^+\Lambda/\Sigma^0$ and $K^-K^+\Lambda/\Sigma^0$ final states in $K^- p$ interactions and 2.5% (95% CL) (Ref. 15) from a comparison of $K^- p \to \pi^-\pi^+\Lambda$ and $K^- p \to K_S^0 K_S^0 \Lambda$.

The suppression of $f' \to \pi\pi$ is analogous to the suppression of $\phi \to \rho\pi$: ϕ and f' are both $\lambda\bar{\lambda}$ states in the quark model and nonstrange decays are suppressed according to the Iizuka-Okubo-Zweig rule.[11] Following Beusch *et al.*[3,4] and Samios *et al.*[30] we estimate

$$\frac{g_{f'\pi\pi}^2}{g_{f\pi\pi}^2} = \frac{\Gamma(f' \to \pi\pi) M_{f'}}{\Gamma(f \to \pi\pi) M_f} \left(\frac{q_\pi(M_f)}{q_\pi(M_{f'})} \right)^5$$

$$= 0.0024 \pm 0.0008 \,. \qquad (7)$$

This is of the same order as the ratio $g_{\phi\rho\pi}^2 / g_{\omega\rho\pi}^2 \lesssim \frac{1}{100}$ estimated by Gaillard, Lee, and Rosner.[38] In fact, for beam momenta of 5 to 6 GeV/c, the ratio $\sigma(\pi^- p \to \phi n)/\sigma(\pi^- p \to \omega n)$ is found[12,39] to be $\sim \frac{1}{300}$. Contrary to the Beusch conclusion that $g_{f'\pi\pi}^2 / g_{f\pi\pi}^2 < \frac{1}{800}$, we do not find much stronger suppression of $f' \to \pi\pi$ than of $\phi \to \rho\pi$.

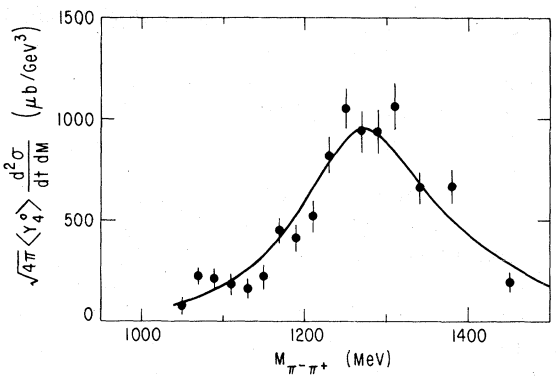

FIG. 25. $\sigma\langle Y_4^0 \rangle$ vs M for the reaction $\pi^- p \to \pi^-\pi^+ n$ at 6 GeV/c and for $0.08 < -t < 0.40$ GeV^2. The curve results from the Breit-Wigner f-meson fit described in the text (χ^2/DF of 34.4/16).

We emphasize that the conclusions about the $f' \to \pi\pi$ branching ratio and 2^{++} nonet mixing angle depend crucially on the assumption that f-f' *interference* for $-t < 0.20$ GeV^2 is due entirely to the OPE mechanism and that f production is dominated by OPE. Note that if both OPE and non-OPE mechanisms contribute to the f' amplitude coherent with the f (i.e., to D_0^{flip}), then our f-f' interference measurement cannot be interpreted even in the sense of a limit on $f' \to \pi\pi$, since the OPE and non-OPE contributions to D_0^{flip} could *a priori* have an arbitrary relative phase.

B. *P*-wave effects

P-wave amplitudes in K^-K^+ appear to be relatively small, and their effects are for the most part observed as interferences with the large $I = 0$ S- and D-wave amplitudes. An exception is

TABLE IV. Mass and width values for the f' from several sources. Note that the results of Refs. 14 and 15 have not been included in the Particle Data Group averaging procedure as yet.

Source	$M_{f'}$ (MeV)	$\Gamma_{f'}$ (MeV)	f-f'-A_2^0 interference effects included?
Particle Data Group (Ref. 13)	1516 ± 3	40 ± 10	No
Brandenburg *et al.* (Ref. 14)	1527 ± 3	61 ± 8	No
ACNO collaboration (Ref. 15) ($K_S^0 K_S^0 \Lambda$ data)	1522 ± 6	62^{+19}_{-14}	No
ACNO collaboration (Ref. 15) ($K^-K^+\Lambda$ data)	1520 ± 13	83 ± 23	Yes
This experiment	1506 ± 5	66 ± 10	Yes

the ϕ meson, which is well localized in mass and only becomes prominent at large $-t$ values.[12, 39]

ϕ meson. Figure 3 shows several hundred $\pi N \to \phi N$ events in the raw event spectra for reactions (1) and (2). The ϕ has a very broad t dependence,[12] $\sim e^{1.6t}$, and as shown in Fig. 4 only becomes prominent in $\sigma_{\rm sum}\langle Y_0^0\rangle$ for $-t \gtrsim 0.20$ GeV^2. Referring to Table II and Fig. 9, we see that the negative values of $\sigma_{\rm sum}\langle Y_2^2\rangle$ in the ϕ bin (1010 $< M <$ 1030 MeV) for $-t > 0.08$ GeV^2 imply a significant natural-parity-exchange production amplitude, P_+; ρ exchange is one obvious candidate for such a mechanism.

Referring again to Table II, we see that the positive signal in $\sigma_{\rm sum}\langle Y_1^0\rangle$ is due to S^*-ϕ interference, with the OPE-produced S^* interfering constructively with a $P_0^{\rm flip}$ ϕ-production amplitude; here B exchange is an obvious possible mechanism. Fits to the mass spectra yielding details on ϕ production from this experiment have been published elsewhere.[39]

$I=1$ P wave. The low-mass $I=1$ P wave is observed via its interference with the S^* (in $\sigma_{\rm dif}\langle Y_1^0\rangle$, Fig. 5) and with the f (in $\sigma_{\rm dif}\langle Y_1^0\rangle$ and $\sigma_{\rm dif}\langle Y_3^0\rangle$, Figs. 5 and 10). Morgan[40] has shown that this P wave is consistent with the tail of the ρ^0 decaying into K^-K^+, with a ρKK coupling that agrees with SU(3), particularly as regards the sign. We have fitted $\sigma_{\rm dif}\langle Y_3^0\rangle$ for $-t < 0.08$ GeV^2 to ρ-f interference, for $M <$ 1450 MeV. At small t OPE dominates and for $M <$ 1450 MeV contributions from the g should be small. We used our standard Breit-Wigner form for the f and took the Roos[41] parameterization of the $\pi^-\pi^+$ P wave, corrected for K^-K^+ phase space and barrier factors,[42, 43]

$$P_0^{\rm flip}(K^-K^+) = \alpha\, P_0^{\rm flip}(\pi^-\pi^+)\left(\frac{q_K}{q_\pi}\right)^{3/2} \times \left(\frac{D_1(q_\pi R_\rho)}{D_1(q_K R_\rho)}\right)^{1/2} \qquad (8)$$

with arbitrary normalization α and using $R_\rho = 3.5$ GeV^{-1}, the same value used for R_f.[1, 28] The overall ρ-f production phase was assumed to be 0°, the SU(3) value.[40, 44] The data are well described by this prescription, as shown by the curve in Fig. 10(j).

We can quantitatively check the SU(3) prediction[44] for the magnitude of $\rho \to K^-K^+$, namely, $\alpha = \frac{1}{2}$ by comparing ρ-f interference in K^-K^+N to that in our companion $\pi^-\pi^+n$ experiment.[20] For K^-K^+N, the ρ-f interference contribution in reactions (1) and (2) is given by $\frac{1}{2}\sigma_{\rm dif}\langle Y_3^0\rangle$ for low masses. We could find the ratio $A \equiv \rho\text{-}f(K^-K^+)/\rho\text{-}f(\pi^-\pi^+)$ immediately if $\sigma_{\pi\pi}\langle Y_3^0\rangle$, the moment for $\pi^- p \to \pi^-\pi^+ n$, were due only to ρ-f interference; however $\sigma_{\pi\pi}\langle Y_5^0\rangle$ shows[8] a significant f-g interference contribution. Empirically, for the region $1040 < M_{\pi\pi} < 1160$ MeV, correcting for f-g interference in $\sigma_{\pi\pi}\langle Y_3^0\rangle$ means using the relation $\rho\text{-}f\ (\pi^-\pi^+) = (1.35 \pm 0.20)\sigma_{\pi\pi}\langle Y_3^0\rangle$. K^-K^+N data have no such effect because the $g \to K^-K^+$ tail is severely damped relative to the $g \to \pi^-\pi^+$ low-mass tail; see Ref. 42 and Sec. IV A. Finally we can determine the experimental value,

$$A_{\rm exp} = \tfrac{1}{2}\sigma_{\rm dif}\langle Y_3^0\rangle/(1.35 \pm 0.20)\sigma_{\pi\pi}\langle Y_3^0\rangle = 0.029 \pm 0.008\,, \qquad (9)$$

where the uncertainty includes a ±10% relative normalization uncertainty between the K^-K^+N and $\pi^-\pi^+n$ experiments. The SU(3) prediction for A, $A_{\rm theor}$, including phase space and barrier factors,[42] is

$$A_{\rm theor} = \frac{1}{2}\left(\frac{q_K}{q_\pi}\right)^{3/2}\left(\frac{D_1(q_\pi R_\rho)}{D_1(q_K R_\rho)}\,\gamma_f(M)\right)^{1/2}, \qquad (10)$$

where $\gamma_f(M)$ is the mass-dependent f branching ratio:

$$\gamma_f(M) = \left(\frac{f \to K^-K^+}{f \to \pi^-\pi^+}\right)_{M=M_f}\left(\frac{q_K q_\pi(M_f)}{q_\pi q_K(M_f)}\right)^5 \times \frac{D_2(q_\pi R_f)D_2(q_K(M_f)R_f)}{D_2(q_K R_f)D_2(q_\pi(M_f)R_f)}\,. \qquad (11)$$

The branching ratio is that measured in this experiment (Sec. IV A above). For the M region centered on 1100 MeV, using $R_f = 3.5$ GeV^{-1} and allowing R_ρ the values 0 to ∞ we obtain the limits

$$0.012 < A_{\rm theor} < 0.027\,, \qquad (12)$$

with a ± 10% overall uncertainty not shown. A value of $R_\rho = 3.5$ GeV^{-1} would imply $A_{\rm theor} = 0.019$. At a level of 1.3 standard deviations, $A_{\rm exp}$ implies $R_\rho \gtrsim 3.5$ GeV^{-1} ($\sim$0.7 Fermi), so the SU(3) prediction and a conventional value of the effective interaction radius successfully predict the relative ρKK vs $\rho\pi\pi$ couplings.

$I=0$ P wave. Apart from the ϕ, no $I=0$ P-wave state coupling to K^-K^+ is known (Emms *et al.*,[32] in their experiment on $\pi^+ n \to \pi^+\pi^-\pi^0 p$, found no evidence for an $I=0$ P wave, other than the ω, which is so narrow and so far below K^-K^+ threshold that we ignore it). If, by analogy with ρ-f interference, we use the f as a probe for an $I=0$ $P_0^{\rm flip}$ amplitude, we should study $\sigma_{\rm sum}\langle Y_3^0\rangle$, Fig. 10. This moment is consistent with zero for $-t < 0.20$ GeV^2 and $M <$ 1200 MeV, and shows a systematic trend to be small and positive for $1200 < M <$ 1500 MeV. For $-t < 0.20$ GeV^2, the small amount of f-A_2^0 interference found in Sec. IV A suggests that the contributions of ρ-A_2^0, A_2^0-g, and f-$\omega(1670)$ interferences to $\sigma_{\rm sum}\langle Y_3^0\rangle$ will be small; whether they will suffice to explain the small signal for 1200 $< M <$ 1500 MeV, or whether an $I=0$ P-wave state

interfering with the f will be required is a question whose resolution must await a detailed model-dependent analysis of the K^-K^+ data.

C. S-wave effects

Low-mass S waves. $\sigma\langle Y_0^0\rangle$, in Fig. 4, shows the well-known near-threshold enhancement, long ascribed to the S^*, an $I=0$ S-wave state[16] coupling strongly to both $\pi\pi$ and $\bar{K}K$ and produced via OPE. For $M \lesssim 1100$ MeV, the non-S-wave contributions to the cross section are known[1] to be small: the P-wave ϕ meson and tail of the ρ^0, and the D-wave low-mass tails of the f and A_2^0 resonances. However $\sigma_{\rm dif}\langle Y_0^0\rangle$ clearly shows a large difference between reactions (1) and (2); for the three t ranges shown in Fig. 4 the ratio σ^+/σ^- increases as $-t$ increases. Figure 26 shows the t distributions for two mass cuts, while Table V gives slopes and intercepts from exponential fits to the data of Fig. 26.

An explanation of this difference is that there are two S-wave amplitudes at low M, one with $I=0$ and the other with $I=1$. The $I=0$ amplitude is presumably the S^* with OPE t dependence, $\sim e^{12t}$, while the $I=1$ amplitude appears to have a much less steep t dependence. To produce the difference between the two reactions at $-t=0.2$ GeV^2, this $I=1$ amplitude must have a component with the same nucleon-helicity-flip behavior as the S^* and magnitude $\gtrsim 20\%$ of the S^*.

Since $\sigma_{\rm sum}$ and $\sigma_{\rm dif}$ have similar mass dependences (in each case, a fast rise from threshold to a plateau), both the $I=0$ and $I=1$ S waves must rise sharply from threshold. This suggests that the $I=1$ S wave be identified with the $\delta^0(970)$ state, which couples strongly to $\eta\pi$ and $\bar{K}K$ and exhibits a threshold enhancement in $\bar{K}K$, as discussed by Flatté[45] in a recent analysis of data[46] on δ^- production. The S^* and δ are known to have similar $\bar{K}K$ mass dependences; see, e.g., Refs. 45–47.

S-wave enhancement under the f meson. A new $\bar{K}K$ S-wave state with mass 1255 ± 5 MeV and width 79 ± 10 MeV was reported by Cason *et al.*,[5] in a recent experiment which studied reaction (3), $\pi^- p \to K_S^0 K_S^0 n$, at 6 and 7 GeV/$c$. The mass and width were determined from one of two phase-shift solutions by using the phase variation with mass given by the S-D interference in the Y_2^0 moment for $-t < 0.2$ GeV^2. Measurement of reaction (3) alone does not determine the isospin I of the S wave. While Cason *et al.* suggest that the effect has $I=1$, we find[48] that the isospin is zero and that the more slowly varying phase solution is preferred, not the rapidly varying Breit-Wigner-type solution which yielded the above values for the mass and width.

In the region $-t < 0.08$ GeV^2, OPE dominates the cross section and in Secs. IV A and IV B we demonstrated our understanding of the small-t P and D waves for masses $M < 1450$ MeV. In this restricted M and t region, we can reliably subtract from $\sigma_{\rm sum}\langle Y_0^0\rangle$ [Fig. 4(g)] the non-S-wave contributions,

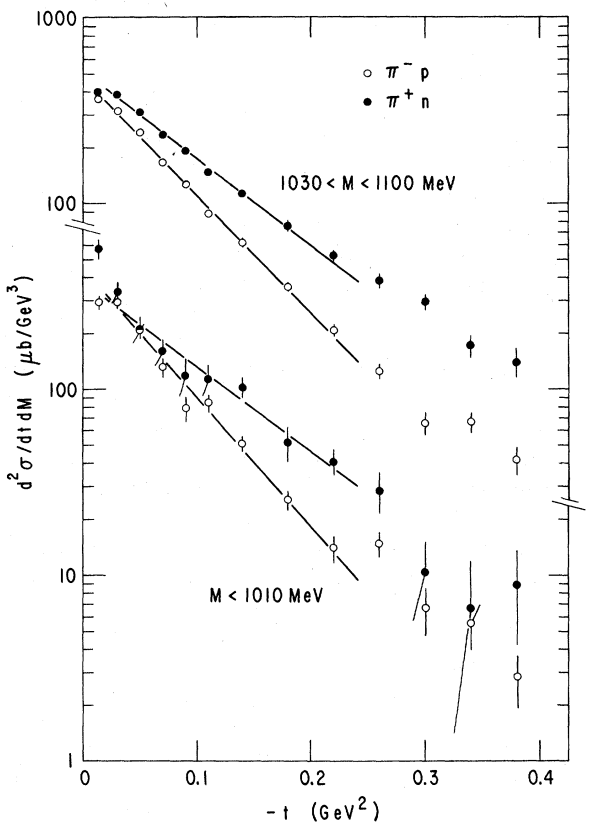

FIG. 26. $\sigma\langle Y_0^0\rangle$ vs t for reactions (1) and (2) in two M ranges at low M. The lines are the result of exponential fits described in the text and in Table V.

TABLE V. Parameters from least-squares fits to t distributions at low mass. The eight data points for $0.02 < -t < 0.24$ GeV^2 are fitted with the two-parameter form $d^2\sigma/dt dM = Ae^{Bt}$, with six degrees of freedom.

	Reaction (1)			Reaction (2)		
M (MeV)	A (μb/GeV^3)	B (GeV^{-2})	χ^2	A (μb/GeV^3)	B (GeV^{-2})	χ^2
<1010	444±24	16.1±0.6	7.9	373±41	10.5±0.9	5.4
1030–1100	476±9	14.8±0.2	10.7	515±17	10.9±0.3	5.0

leaving

$$\sigma^{S}_{\text{sum}}\langle Y^0_0\rangle = 2(|I=0\ S\ \text{wave}|^2 + |I=1\ S\ \text{wave}|^2)\ .$$

The f, f', and $I=1$ P wave were assumed to have the absorbed OPE production mechanism which is well known, while the A_2^0 contribution was an extrapolation (as p_{lab}^{-2}) of the 4-GeV/c data of Emms *et al.*[32] Below 1450 MeV, spin ≥ 3 effects are negligible. The result of the subtraction is shown in Fig. 27. The error bars shown are just the statistical errors on $\sigma_{\text{sum}}\langle Y^0_0\rangle$, since the smooth mass dependence of the subtraction introduced no point-to-point jitter. The S^* peak below 1100 MeV is clearly exhibited, as well as a second peak of mass ~1300 MeV and width ~150 MeV. Note that S wave accounts for nearly half of the cross section at 1300 MeV. The systematic uncertainty in $\sigma^{S}_{\text{sum}}\langle Y^0_0\rangle$ is about $\pm 10\%$ at 1300 MeV.

The Y^0_2 moments for all three reactions (1 to 3) are very similar at small momentum transfer, as shown in Fig. 7. Below 1200 MeV these moments are dominated by a negative S-D interference, while above 1200 MeV the positive $|D|^2$ term from the f meson becomes dominant. For $-t < 0.08$ GeV^2 the S-D interference seen in Y^0_2 near 1200 MeV is about three times larger in the sum spectrum than in the difference spectrum. Since the D-wave cross section is mainly $I=0$ at small t, the Y^0_2 moments suggest that the $I=0$ part of the S-wave cross section shown in Fig. 27 is of order 10 times the $I=1$ contribution.

To investigate this in more detail, we have used the same assumptions as those made in Ref. 5 to perform an amplitude analysis[49] of the K^-K^+ system produced in reactions (1) and (2) for $-t$

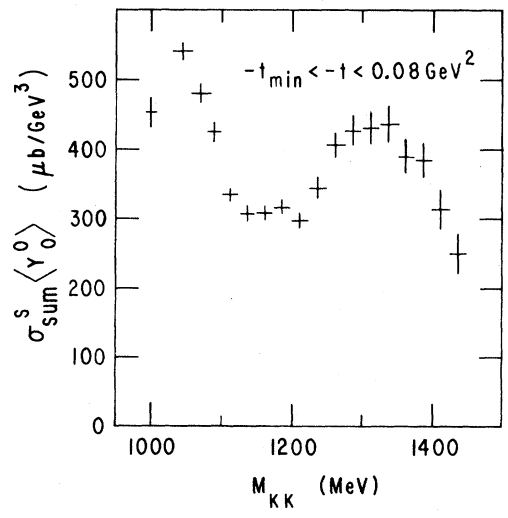

FIG. 27. The S-wave contributions to $\sigma_{\text{sum}}\langle Y^0_0\rangle$ at small t, for $M < 1450$ MeV, resulting from the subtraction procedure described in the text.

≤ 0.08 GeV^2. For each reaction there is a four-fold ambiguity in the partial-wave amplitudes, two solutions giving the S-wave enhancement near 1300 MeV, and the remaining pair giving a large P-wave amplitude in this region. The latter solutions can be rejected in a model-independent way for reaction (2), since they are incompatible[50] with the results from reaction (3).

By choosing the P-wave solution to be that expected theoretically, we can resolve the remaining ambiguities. As discussed above, the P wave is consistent with the tail of the ρ^0 decaying into K^-K^+, with a ρKK coupling that agrees with SU(3), including the sign. Only one of the ambiguous solutions corresponds to the SU(3) prediction, and the others can all be rejected since they result in very different P-wave amplitudes. The one remaining solution was used to calculate the S-wave cross section shown in Fig. 27 and leads to a dominantly $I=0$ S wave with values of $|\varphi_D - \varphi_S|$ in good agreement with those found by Cason *et al.*[5] It further resolves the ambiguity of the sign of the difference between φ_D and φ_S in favor of the slow steady variation of the S-wave phase shown by "solution 2" of Cason *et al.* Since other solutions do not give the P-wave behavior expected, we conclude that the solution with a large $I=0$ S wave and slowly varying phase is by far the preferred solution.

In their amplitude analysis Cason *et al.* found a relatively shallow t dependence for the S-wave cross section, a slope of 3.7 ± 0.8 GeV^{-2} in the mass range 1.22 to 1.32 GeV, compared with 11.9 ± 1.2 GeV^{-2} for the D wave. This was used to argue that OPE was not important for the S-wave enhancement, and that it therefore had odd-G parity and $I=1$. The cross sections for our two reactions (1) and (2) show a difference in slope indicating that both $I=0$ and $I=1$ waves are important at large t [Fig. 4 (j)–(l), Fig. 22, and Fig. 28]. Since the $\sigma\langle Y^0_4\rangle$ moments do not show a difference, this is not a D-wave effect, but is primarily due to interference in the S-wave amplitudes. The slope of the S-wave cross section observed in any one reaction is then difficult to interpret, since it is due to a coherent sum of the $I=0$ and $I=1$ amplitudes. The interpretation of the slope is further complicated by the fact that the assumptions required for the amplitude analysis may not be valid at large t where terms other than OPE (e.g., A_2^0 production) can become important. The t dependence of the negative S-D interference in $\sigma_{\text{sum}}\langle Y^0_2\rangle$, where the negative signal near 1200 MeV becomes less prominent at large t, is consistent (in the limit that the f dominates the D wave) with OPE-like t dependence for the $I=0$ S wave. On the other hand, $\sigma_{\text{dif}}\langle Y^0_2\rangle$, with a slope $B \sim 4$ GeV^{-2}, implies a much broader t dependence than OPE

for the $I=1$ S wave in the 1200–1250 MeV region. In fact, as Fig. 28 shows, $\sigma_{\rm dif}\langle Y_2^0\rangle$ for 1200–1250 MeV has a similar t dependence to $\sigma_{\rm dif}\langle Y_0^0\rangle$ for 1030–1100 MeV; this suggests identifying each as due to interference of the $I=1$ $\delta^0(970)$ with an $I=0$ OPE-produced state: $S^*-\delta$ for Y_0^0 and f-δ for Y_2^0. We conclude that, while the dominant S wave for $-t<0.08$ GeV^2 has $I=0$, the $I=1$ S wave becomes important as well at larger t. In consequence, the $\sim e^{4t}$ behavior of $|S|^2$ found by Cason *et al.*[5] cannot be interpreted as the t dependence of a single S-wave state of definite isospin.

With $I=0$, the small-t enhancement in $\sigma^S_{\rm sum}\langle Y_0^0\rangle$ around 1300 MeV has the same quantum numbers as the S^*, namely $I^G J^{PC}=0^+0^{++}$, and we refer to this enhancement as the S'. Since the S^* and S' can interfere with one another, the $\sigma^S_{\rm sum}\langle Y_0^0\rangle$ spectrum should not be interpreted in terms of two incoherent peaks. Indeed, the slow phase variation of our solution argues against interpretation in terms of a narrow S' state. Using Flatté's parameterization[47] of the S^* with $M\approx 960$ MeV and $\Gamma\approx 100$ MeV, we find that the intensity and phase of the total $I=0$ S wave can be described by adding to the S^* a very slowly varying S' amplitude. The intensity minimum in $\sigma^S_{\rm sum}\langle Y_0^0\rangle$ around 1150 MeV is caused by destructive interference between the S^* (Im$S^*>0$) and the S' (near-constant S' phase $\sim 270°$). The properties of the S' would then be consistent with the broad ϵ effect seen in $\pi\pi\to\pi\pi$ in this mass region,[8,51] the ϵ having a negative coupling to K^-K^+ relative to $\pi^-\pi^+$. This explanation is of course not unique since the mass and width of the S^* are uncertain. We should also point out that with its large coupling to $\bar{K}K$, the S' does not fit well into a conventional SU(3) framework in which this decay would be strongly suppressed.[51]

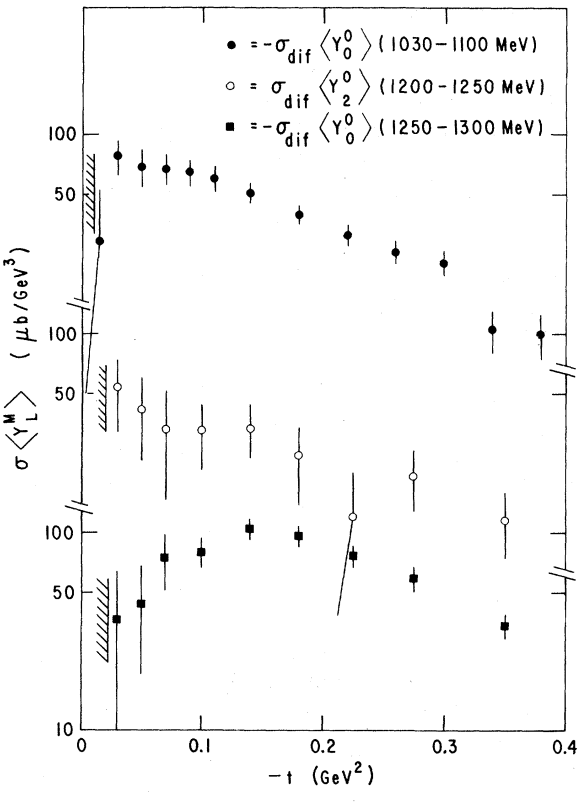

FIG. 28. Momentum-transfer distributions for several difference moments in the indicated mass ranges.

V. SUMMARY

The Effective Mass Spectrometer was used to accumulate a sample of 110000 events of the reaction $\pi^- p\to K^-K^+n$ and 50000 events of the companion reaction $\pi^+ n\to K^-K^+p$ at 6 GeV/c. For K^-K^+ masses below 1750 MeV and $-t<0.4$ GeV^2 the angular distributions of the K^-K^+ system were parameterized in terms of t-channel moments, and the results are shown as functions of K^-K^+ mass in Figs. 4–21 for three invervals of t. The moments are also available in tabular form.[25]

Interferences between K^-K^+ states of $I=0$ with those of $I=1$ change sign going from the π^-- to the π^+-induced reaction. These interference terms can thus be isolated by taking the differences between the unnormalized moments of the two reactions, while they are canceled in the sum of the moments; these sums and differences are also shown in Figs. 4–21.

One-pion exchange (OPE) is dominant in these reactions at small t. The $m=0$ moments dominate over those with $m=1$, while the $m=2$ moments are generally smaller still; such features have been observed[8] in studies of the OPE-dominated reaction $\pi^- p\to\pi^-\pi^+ n$. OPE produces K^-K^+ states with even-G parity; the statistics of boson-antiboson pairs require such states to have $I=0$ for even spin and $I=1$ for odd spin. This is reflected in the moments: The even moments are roughly the same for the two reactions, while the odd moments are approximately mirror images in the two cases. Non-OPE amplitudes become increasingly important at large t and result in a substantial difference between the slopes of the two reactions (Fig. 22).

The moments are most easily understood by starting with the highest important moment, Y_4^0, which is dominated by the D wave, and then considering the P wave and S wave in the lower moments once the D wave is understood. The mass dependence of the Y_4^0 moments was well fitted by a sum of the $f(1270)$, A_2^0, and f' Breit-Wigner shapes and their interference. The f dominates

Y_4^0 at low t in the mass region below 1500 MeV. Comparison with Y_4^0 from a previous $\pi^- p \to \pi^- \pi^+ n$ experiment gave the branching ratio $(f \to \bar{K}K)/(f \to \text{all}) = (3.8 \pm 0.4)\%$.

The presence of $f'(1514)$ production was demonstrated here for the first time in pion-induced reactions. It was observed as interferences with the tails of the f and A_2^0 resonances, the interference producing in the π^--induced reaction a striking falloff in Y_4^0 near 1500 MeV. The f' production amplitude was found to be real relative to the f amplitude $[\varphi_f - \varphi_{f'} = (170 \pm 10)^\circ]$, as expected for OPE. Assuming that the f-f' interference term is due to OPE, we found $(f' \to \pi\pi)/(f' \to \text{all}) = (1.2 \pm 0.4)\%$. This is somewhat above the upper limit of 0.9% obtained from a study[3] of the reaction $\pi^- p \to K_S^0 K_S^0 n$, which is closely related to reaction (2) by charge independence. The lack of a large f' effect in these reactions is explained by a cancellation between the f'-f and f'-A_2^0 interference terms. The coupling $f' \to \pi\pi$ is presumably strongly suppressed by the Iizuka-Okubo-Zweig rule[11] since the f', like the ϕ, is a $\lambda\bar{\lambda}$ state in the quark model; we find $g^2(f' \to \pi\pi)/g^2(f \to \pi\pi) \sim \frac{1}{400}$, about the same as found for $g^2(\phi\rho\pi)/g^2(\omega\rho\pi)$. The fit to the Y_4^0 moments also gave $M_{f'} = 1506 \pm 5$ MeV and $\Gamma_{f'} = 66 \pm 10$ MeV.

Very little f-A_2^0 interference was observed. This indicates that the unnatural-parity-exchange amplitudes for A_2^0 production are largely incoherent with the OPE f amplitude because of a different coupling to the nucleon spin (e.g., Z exchange). Some f-A_2^0 interference is observed in the $-t$ interval 0.2 to 0.4 GeV^2 with a relative production phase of $(63^{+11}_{-15})^\circ$ in good agreement with the Irving and Michael[28] prediction of $\sim 70^\circ$.

With the exception of the φ meson, the P wave is consistent with that expected from the tail of the $I=1$ ρ meson. In the mass region 1040–1160 MeV the Y_3^0 moment for K^-K^+ is dominated by ρ-f interference; it was compared to that for $\pi^-\pi^+$: ρ-$f(K^-K^+)/\rho$-$f(\pi^-\pi^+) = 0.029 \pm 0.008$ consistent with the value of 0.019 predicted by SU(3) (assuming an effective interaction radius $R_\rho = 3.5$ GeV^{-1}). The ϕ has a very broad t dependence and is discussed in a separate paper.[39]

Near threshold the S wave is dominated by the OPE-produced S^*. The $I=1$ δ is important at large t and changes the cross-section slope for the mass region 1030 to 1100 MeV from 14.8 ± 0.2 GeV^{-2} for the $\pi^- p$ reaction to 10.9 ± 0.3 GeV^{-2} for the $\pi^+ n$ reaction. A difference in slope for the two reactions, mainly due to S-wave effects, persists up to a mass of 1400 MeV (Fig. 22).

The S-wave cross section was obtained by assuming that the P wave is dominated by the ρ tail; this assumption was required to resolve the discrete ambiguities. In addition to the S^* peak below 1100 MeV, Fig. 27 shows a second peak of mass ~1300 MeV and width ~150 MeV. While this structure was not shown by an analysis of the $K_S^0 K_S^0$ experiment of Beusch *et al.*,[3,4] it is very similar to that found in the recent $K_S^0 K_S^0$ experiment of Cason *et al.*[5] The requirement of a reasonable P-wave solution (a constraint unavailable to $K_S^0 K_S^0$ analyses) resolves the phase-shift ambiguity of Cason *et al.* in favor of the slow, steady variation of the S-wave phases shown by their "solution 2." It also shows that the S wave is dominantly $I=0$, consistent with the broad ϵ effect seen in $\pi\pi \to \pi\pi$ in this mass region. This excludes the interpretation of Cason *et al.* that the S-wave enhancement at 1300 MeV is a narrow $I=1$ state.

ACKNOWLEDGMENTS

The spectrometer was designed and constructed in collaboration with I. Ambats, A. F. Greene, A. Lesnik, D. R. Rust, C. E. W. Ward, and D. D. Yovanovitch. R. Diaz, L. Filips, and E. Walschon were instrumental in the construction and maintenance of the spectrometer. We are grateful to Professor R. Winston of the University of Chicago for the loan of the large Čerenkov counter and are indebted to the Zero Gradient Synchrotron personnel for their support during all phases of the experiment. We thank H. J. Lipkin for suggesting consideration of f' effects in our data. We thank E. Lorenz,[2] W. Beusch,[3,4] and N. Cason[5] for privately communicating preliminary data on their experiments and for useful conversations.

*Work supported by the U. S. Energy Research and Development Administration.

[1]A. J. Pawlicki *et al.*, Phys. Rev. D 12, 631 (1975).
[2]W. Blum *et al.*, Phys. Lett. 57B, 403 (1975).
[3]W. Beusch *et al.*, Phys. Lett. 60B, 101 (1975).
[4]W. Wetzel *et al.*, Nucl. Phys. B115, 208 (1976).
[5]N. M. Cason *et al.*, Phys. Rev. Lett. 36, 1485 (1976).
[6]H. J. Lipkin, Phys. Rev. 176, 1709 (1968).
[7]See for example Particle Data Group, Rev. Mod. Phys. 41, 109 (1969), especially p. 115.
[8]G. Grayer *et al.*, Nucl. Phys. B75, 189 (1974).
[9]A. D. Martin and C. Michael, Nucl. Phys. B84, 83 (1975).
[10]A. J. Pawlicki *et al.*, Phys. Rev. Lett. 37, 971 (1976).
[11]I. Iizuka, Prog. Theor. Phys. Suppl. 37–38, 21 (1966); S. Okubo, Phys. Lett. 5, 165 (1963); G. Zweig, CERN Report No. TH. 412, 1964 (unpublished).
[12]D. S. Ayres *et al.*, Phys. Rev. Lett. 32, 1463 (1974).

[13]Particle Data Group, Rev. Mod. Phys. 48, S1 (1976).
[14]G. W. Brandenburg *et al.*, Nucl. Phys. B104, 413 (1976).
[15]Amsterdam-CERN-Nijmegen-Oxford Collaboration, CERN Report No. CERN/EP/PHYS 76-26 (unpublished).
[16]G. Grayer *et al.*, in *π-π Scattering—1973*, proceedings of the International Conference on π-π Scattering and Associated Topics, Tallahassee, 1973, edited by P. K. Williams and V. Hagopian (AIP, New York, 1973), p. 117; S. D. Protopopescu *et al.*, Phys. Rev. D 7, 1279 (1973).
[17]A. J. Pawlicki *et al.*, Phys. Rev. Lett. 31, 665 (1973).
[18]I. Ambats *et al.*, Phys. Rev. D 9, 1179 (1974); D. S. Ayres, in *Proceedings of the International Conference on Instrumentation for High Energy Physics, Frascati, Italy, 1973*, edited by S. Stipcich (Laboratori Nazionali del Comitato Nazionale per l'Energia Nucleare, Frascati, Italy, 1973), p. 665.
[19]H. Hinterberger *et al.*, Rev. Sci. Instrum. 41, 413 (1970).
[20]S. L. Kramer *et al.*, Phys. Rev. Lett. 33, 505 (1974); A. B. Wicklund *et al.*,(unpublished).
[21]We have parameterized the deuteron form-factor data of Ref. 22 as $S(\Delta) = \exp(43t + 110t^2)$, $-t < 0.20$ GeV^2, and $S(\Delta) = 0$ for $-t \geq 0.20$ GeV^2.
[22]J. Elias *et al.*, Phys. Rev. 177, 2075 (1969); J. A. McIntyre *et al.*, *ibid.* 106, 1074 (1957).
[23]P. Fleury, in *Methods in Subnuclear Physics*, edited by M. Nikolic (Gordon and Breach, New York, 1968), Vol. II, p. 541.
[24]A. Dar and A. Gal, Phys. Rev. Lett. 21, 444 (1968).
[25]Tables of the moments are available from the authors.
[26]P. Estabrooks *et al.*, in *π-π Scattering—1973*, proceedings of the International Conference on π-π Scattering and Associated Topics, Tallahassee, 1973, edited by P. K. Williams and V. Hagopian (AIP, New York, 1973), p. 37.
[27]Our $B(M)$ are the $D(M)$ functions defined in Ref. 1. The masses and widths used are (in MeV) $M_f = 1279$, $\Gamma_f = 202$, $M_{A_2} = 1310$, $\Gamma_{A_2} = 104$. The f' mass and width were treated as free parameters.
[28]A. C. Irving and C. Michael, Nucl. Phys. B82, 282 (1974).
[29]The Q_k coefficients are averages over the finite t interval used. For $-t < 0.08$ GeV^2, $t_{\min}$ varies significantly with mass, hence the t interval averaged over is mass-dependent and we cannot do this type of analysis. We have omitted the effects of P-F interference. Analysis of the Y_3^0 moment (Sec. IV B) revealed no $I = 0$ P wave (other than the ϕ meson), while the $I = 1$ P wave was just the $\pi^-\pi^+$ P wave, corrected for K^-K^+ decay phase space. In the F waves, the g meson ($I = 1$) is expected to dominate over the $I = 0$ $\omega(1670)$ meson, so the only significant P and F waves have isospin 1 and their interference contributes to $\sigma_{\text{sum}} \langle Y_4^0 \rangle$. As an example of the size of the neglected contribution, Fig. 13(g) shows the estimated contribution for $-t < 0.08$ GeV^2. The t dependence of this contribution should be that of OPE.
[30]N. P. Samios *et al.*, Rev. Mod. Phys. 46, 49 (1974).
[31]A. C. Irving, Nucl. Phys. B105, 491 (1976).
[32]M. J. Emms *et al.*, Phys. Lett. 58B, 117 (1975); 60B, 109 (1975).
[33]The absolute mass scale is known to ±2 MeV and the effective mass resolution is ±3 MeV at 1500 MeV.
[34]For example, in $\bar{K}N \to \bar{K}K\Lambda$, $\bar{K}K\Sigma^0$, if $f, f' - A_2^0$ all had the same production phase, then the Breit-Wigner phases would give destructive f-f' and f'-A_2^0 interferences below the f' central mass, shifting the apparent f' peak to higher mass and narrower width.
[35]H. J. Lipkin, private communication and Nucl. Phys. B7, 321 (1968).
[36]G. Alexander *et al.*, Phys. Rev. Lett. 17, 412 (1966).
[37]This value differs slightly from that given in Ref. 10 for two reasons. First, a factor of $M_{f'}/M_f$ in Eq. (6) was inadvertently inverted in the computation in Ref. 10; second, we now use the value ($f \to \bar{K}K/f \to$ all) determined from this experiment rather than the value found in our previous experiment (Ref. 1) in evaluating Eq. (6).
[38]M. K. Gaillard, B. W. Lee, and J. L Rosner, Rev. Mod. Phys. 47, 277 (1975).
[39]D. Cohen *et al.*, Phys. Rev. Lett. 38, 269 (1977).
[40]D. Morgan, Phys. Lett. 51B, 71 (1974).
[41]M. Roos, Nucl. Phys. B97, 165 (1975).
[42]Following Refs. 8, 28, and 43, we write the phase space and barrier factor dependence of a $K^-K^+/\pi^-\pi^+$ decay branching ratio of a spin L meson as $K^-K^+/\pi^-\pi^+ \propto (q_K/q_\pi)^{2L+1} D_L(q_\pi R)/D_L(q_K R)$, where the $D_L(x)$ are related to the spherical Hankel functions. The decay momentum q is in GeV/c the radius R in GeV^{-1}. The $D_L(x)$, $L \leq 4$, are $D_0(x) = 1$, $D_1(x) = x^2 + 1$, $D_2(x) = x^4 + 3x^2 + 9$, $D_3(x) = x^6 + 6x^4 + 45x^2 + 225$, $D_4(x) = x^8 + 10x^6 + 135x^4 + 1575x^2 + 11\,025$. Thus, the modified SU(3) prediction is

$$\frac{\rho \to K^-K^+}{\rho \to \pi^-\pi^+} = \frac{1}{4}\left(\frac{q_K}{q_\pi}\right)^3 \frac{D_1(q_\pi R)}{D_1(q_K R)} .$$

As $R \to 0(\infty)$, the lower (upper) limit of the ratio is approached.
[43]F. von Hippel and C. Quigg, Phys. Rev. D 5, 624 (1972).
[44]C. Sorensen, private communication.
[45]S. M. Flatté, Phys. Lett. 63B, 224 (1976).
[46]J. B. Gay *et al.*, Phys. Lett. 63B, 220 (1976).
[47]S. M. Flatté, Phys. Lett. 63B, 228 (1976).
[48]A. J. Pawlicki *et al.*, Phys. Rev. Lett. 37, 1666 (1976).
[49]D. Cohen *et al.*, (unpublished).
[50]For example, near 1300 MeV the large P-wave solutions would predict a difference in $\sigma \langle Y_2^0 \rangle$ between reactions (2) and (3) of 140 μb/GeV^3 in Fig. 7(d), an effect clearly ruled out by the data.
[51]D. Morgan, in *New Directions in Hadron Spectroscopy*, edited by S. L. Kramer and E. L. Berger (ANL, Argonne, Illinois, 1975), p. 45.